Aus der Klinik für Anaesthesiologie
Klinik der Universität München
Direktor: Prof. Dr. Bernhard Zwißler

Differential effects of acute and chronic hydrocortisone treatment on pyroptosis *in vitro*

Dissertation
zum Erwerb des Doktorgrades der Medizin
an der Medizinischen Fakultät der
Ludwig-Maximilians-Universität zu München

vorgelegt von
Bing Han

aus

Wuhan, Hubei, Volksrepublik China

Jahr

2023

Mit Genehmigung der Medizinischen Fakultät
der Universität München

Berichterstatter:	Prof. Dr. med. Alexander Choukér
Mitberichterstatter:	Prof. Dr. Rainer Haas
	PD Dr. Dimitrios Frangoulidis
Mitbetreuung durch den promovierten Mitarbeiter:	Dr. rer. nat. Dominique Moser
Dekan:	Prof. Dr. med. Thomas Gudermann
Tag der mündlichen Prüfung:	13.07.2023

Table of content

Zusammenfassung (Deutsch):

Die Pyroptose ist eine Form des entzündungsverursachenden programmierten Zelltodes, der durch PAMPs (*Pathogen Associated Molecular Patterns* / Pathogen-assoziierte molekulare Muster) von pathologischen Mikroben und intrazellulären Komponenten von geschädigten Zellen ausgelöst wird. Dadurch sollen Immunzellen angelockt und die Ausbreitung einer Infektion verhindert werden. Pyroptose findet hauptsächlich in Makrophagen statt, kann aber auch in anderen Immunzellen und Epithelzellen auftreten. Nach einer PAMP-Stimulation wird der proinflammatorische NF-κB-Signalweg aktiviert, was die Assemblierung des Inflammasoms und die Spaltung der Effektor-Caspase-1 zur Folge hat. Die Hauptmerkmale der Pyroptose sind eine durch Gasdermin D-Poren vermittelte Zelllyse und die Freisetzung der entzündungsfördernden Zytokine IL-1β und IL-18 in den extrazellulären Raum.

Das weitläufig verabreichte synthetische Glucocortikoid (GC) Hydrocortison (HC) ist ein steroidales Medikament zur Behandlung von schweren Entzündungen. Physiologisch werden GCs bei Stress aus der Nebennierenrinde sezerniert und wirken als Immunsuppressivum und entzündungshemmendes Hormon, indem sie entzündungsfördernde Signalwege (z. B. NF-κB) hemmen. Für HC wurde jedoch gezeigt, dass es auch das Potenzial hat, entzündungsfördernde Gene wie TLRs (Toll-like-Rezeptoren) und NLRP3 hochzuregulieren, was darauf hindeutet, dass HC sowohl positive als auch negative Auswirkungen auf die Entzündungsreaktion haben kann. Der Einfluss von HC auf die Pyroptose in Makrophagen wurde bisher nicht adressiert.

In der vorliegenden Arbeit wurden die Auswirkungen einer Erhöhung der HC-Konzentrationen auf die Induktion und Ausführung der Pyroptose in THP-1-Makrophagen untersucht. Hierfür wurden die Zellen mit 0,1 µg/ml HC vorbehandelt, um basale Cortisolspiegel nachzuahmen, oder mit 0,2 und 0,4 µg/ml für chronisch erhöhte Konzentrationsspiegel. Pyroptose wurde durch LPS (Lipopolysaccharid, 5 ng/ml) und ATP (Adenosintriphosphat, 5 mM) induziert. Die weitere Behandlung mit HC nach Pyroptoseinduktion erfolgte als eine akute Erhöhung von 0,1 µg/ml auf 0,2 bzw. 0,4 µg/ml, die Konzentrationen einer klinischen Bedingung bei der Behandlung von schweren Infektion entsprechen bzw. bei mäßig (0,2

µg/ml) oder stark (0,4 µg/ml) gestressten oder mit HC vorbehandelten Patienten auftreten können.

Die Ergebnisse der Untersuchungen haben gezeigt, dass eine akute HC-Exposition die LPS- und ATP-vermittelte pyroptotische Zelllyse im Vergleich zur physiologischen Kontrolle nicht veränderte, jedoch eine chronische erhöhte HC-Exposition die Zelllyse dosisabhängig verminderte. Interessanterweise waren nach akuter HC-Exposition die NLRP3- und Caspase-1-Aktivierung sowie die extrazellulären IL-1β-Spiegel dosisabhängig erhöht. Die Aktivierung des NF-κB-Signalweges und die IL-1β-mRNA-Spiegel blieben jedoch unter diesen Bedingungen unverändert. Die chronische Exposition hingegen unterdrückte den NF-κB-Signalweg, die Proteinexpression und deren Aktivierung. Die Ergebnisse dieser Untersuchungen zeigen, dass in Abhängigkeit einer akuten oder chronischen Exposition die Effekte von HC auf die Pyroptose und die Ausschüttung des pro-inflammatorischen Zytokins IL-1β unterschiedlich ausfallen. Sie legen zudem die Umsetzung klinischer Studien zur Bewertung der Auswirkungen von IL-1β als möglichen Entzündungs- und pharmakologischen Biomarker für den klinischen Alltag nahe.

Abstract (English):

Pyroptosis is a mode of inflammatory programmed cell death triggered by Pathogen Associated Molecular Patterns (PAMP) of pathological microbes and intracellular components from damaged cells in order to attract immune cells and to prevent spread of infection. Pyroptosis occurs mostly in macrophages but can be also found in other immune cells and epithelial cells. Upon PAMP-stimulation the pro-inflammatory NF-κB signaling pathway is activated, which is followed by inflammasome assembly and cleavage of effector caspase-1. The main features of pyroptosis are cell lysis mediated by gasdermin D pores, and release of the pro-inflammatory cytokines IL-1β and IL-18 into the extracellular space.

The widely used synthetical glucocorticoid (GC) hydrocortisone (HC) is a steroidal drug to limit inflammation. Physiologically, GCs are secreted from the adrenal cortex upon stress and act as immune suppressants and anti-inflammatory hormones by inhibiting pro-inflammatory signaling pathways (e.g. NF-κB). However, it was shown that HC also has the potential to upregulate pro-inflammatory genes such as TLRs (Toll like receptors) and NLRP3, which indicates that HC can have both positive and negative effects on inflammatory immune responses. The impact of HC on pyroptosis in macrophages was not addressed by now.

In the present work, the effects of incrementing HC concentrations on induction and execution of pyroptosis were investigated in THP-1 macrophage-like cells. Accordingly, cells were pre-treated either with 0.1 µg/ml HC to mimic basal human cortisol levels or with 0.2 and 0.4 µg/ml to mimic chronically increased concentration levels. Pyroptosis was induced by LPS (lipopolysaccharide, 5 ng/ml) and ATP (adenosine triphosphate, 5 mM). Subsequent treatment with HC after pyroptosis induction was scheduled as an acute concentration increase from 0.1 µg/ml to 0.2 or 0.4 µg/ml, which corresponds to patients HC treatment upon severe inflammation or constant moderately (0.2 µg/ml) or highly (0.4 µg/ml) elevated HC levels, resembling stress condition or patients otherwise pretreated with HC, respectively.

Results derived from these investigations have shown, that the acute HC exposure did not change LPS- and ATP-mediated cell lysis compared to physiological control, however chronically elevated HC dose-dependently attenuated cell lysis.

Interestingly, after acute exposure, NLRP3 and caspase-1 activation as well as extracellular IL-1β levels were dose-dependently augmented. However, NF-κB signaling pathway activation and IL-1β mRNA levels were unaltered under these conditions. Chronic exposure suppressed the NF-κB signaling pathway, protein expression and their activation.

This study described that the effects of HC on pyroptosis in macrophages as well as on their release of the proinflammatory cytokine IL-1β are differently affected in dependence of an acute or chronic HC exposure. Moreover, the data promotes potential clinical studies to evaluate the impact of IL-1β as a possible inflammation and pharmacological biomarker in daily clinical routine.

List of figures

List of tables

List of abbreviations

APC	Allophycocyanin
APCs	Antigen presenting cells
APS	Ammonium persulfate
ASC	Apoptosis-associated speck-like protein containing a CARD
ATP	Adenosine 5'-triphosphate
BSA	Bovine serum albumin
CD	Cluster of differentiation
CST	Cell Signaling Technology
DAPI	4',6-diamidino-2-phenylindole
DMSO	Dimethyl sulfoxide
DTT	Dithiothreitol
ELISA	Enzyme-linked immunosorbent assay
FBS	Fetal bovine serum
FITC	Fluorescein isothiocyanate
g	gravitational acceleration
GAPDH	Glyceraldehyde 3-phosphate dehydrogenase
HC	Hydrocortisone
HCl	Hydrochloric acid
IFN	Interferone
IL	Interleukin
LDH	Lactate dehydrogenase
LPS	Lipopolysaccharide
min	minute(s)
ml	milliliter
NC	Nitrocellulose
NF-κB	nuclear factor kappa-light-chain-enhancer of activated B cells
NLRP3	NLR family pyrin domain containing 3
P/S	Penicillin-streptomycin
PAMP	Pathogen associated molecular pattern
PBS	Phosphate-buffered saline
PMA	Phorbal 12-myristate 13-acetate
PRR	Pattern recognition receptor
RPMI	Roswell Park Memorial Institute
SDS	Sodium dodecyl sulfonate
TBS	Tris-buffered saline
TBS-T	Tris-buffered saline with 0.1 % tween 20
TEMED	N,N,N',N'-Tetramethylethylenediamine
TLR	Toll-like recptor
TNF	Tumor necrosis factor
µg	microgram
µl	microliter

1. Introduction

1.1 Effector cells of the mononuclear phagocyte system: monocytes and macrophages

The mononuclear phagocyte system is a part of the innate immune system that consists of phagocytic cells, primarily of monocytes and macrophages. Monocytes are representatives of the myeloid-originated cellular branch of the innate immune system and comprise 5~10% of peripheral leukocytes in humans (Gordon & Taylor, 2005). Their main functions are phagocytosis and antigen-presentation (Jakubzick, Randolph, & Henson, 2017). According to their surface markers, human monocytes are distinguished into classical monocytes ($CD14^{++}$ $CD16^{low}$), intermediate monocytes ($CD14^{++}$ $CD16^{+}$) and non-classical monocytes ($CD14^{low}$ $CD16^{+}$). Classical monocytes migrate immediately to inflamed/infected tissue and exhibit phagocytic and pro-inflammatory functions; intermediate monocytes carry out pro-inflammatory and antigen-presenting functions; non-classical monocytes patrol the vasculature to remove cell debris and repair the endothelium during homeostasis (Randolph, Beaulieu, Lebecque, Steinman, & Muller, 1998; Sampath, Moideen, Ranganathan, & Bethunaickan, 2018; Wolf, Yáñez, Barman, & Goodridge, 2019). Monocytes generally have the ability to produce and to respond to pro- and anti-inflammatory signals such as cytokines, and upon inflammation they are recruited by chemotactic cytokines (chemokines) to emigrate into affected tissue and to differentiate into macrophages (Janssen et al., 2011).

Macrophages were considered to derive exclusively from monocytes, however, recent research shows that some macrophages already developed during embryogenesis and emigrated from yolk sac and fetal liver into tissues. These macrophages are called tissue-resident macrophages and their amount decreases to a low percentage after birth, but they are able to renew themselves in respective tissues (Ginhoux & Jung, 2014). Monocyte-derived macrophages are classified into pro-inflammatory macrophages (M1 macrophage) and pro-resolving macrophages (M2 macrophage). M1 macrophages are associated with inflammatory processes and can be stimulated by Interferone (IFN)-γ or lipopolysaccharide

(LPS). They highly express the surface molecules CD80 and CD86 to stimulate lymphocyte activation and pro-inflammatory cytokines such as Interleukin (IL) -6 and tumor necrosis factor (TNF). M2 macrophages can be differentiated by IL-4 (Orecchioni, Ghosheh, Pramod, & Ley, 2019; Yunna, Mengru, Lei, & Weidong, 2020) and express CD206, Arg-1 and anti-inflammatory cytokines such as IL-10 to support tissue repair (Jakubzick et al., 2017).

Being cells of the MPS, macrophages eliminate microorganisms and remove cell debris by phagocytosis within tissues. They release pro-inflammatory cytokines such as IL-1β, TNF and IFN-γ to recruit other innate or adaptive immune cells to fight infection. Moreover, macrophages are like monocytes but also like dendritic cells and B cells professional antigen-presenting cells (APCs). They constitutively express MHC-II molecules to present internalized and processed antigens to T-helper cells in order to initiate, modulate and resolve inflammation (Hohl et al., 2009; Kashem, Haniffa, & Kaplan, 2017).

Thus, monocytes and macrophages play a central role in innate immunity during infection and represent a bridge between the innate and adaptive immune system.

1.2 Toll-like receptors on monocytes and macrophages

To recognize antigens such as conserved pathogenic microbial products or pathogen associated molecular patterns (PAMPs), monocytes and macrophages express a variety of pattern recognition receptors (PRR) including RIG-I–like receptors, C-type lectin receptors and Toll-like receptors (TLRs) (Fitzgerald & Kagan, 2020). By now, 10 different TLRs have been identified in humans. TLRs 1, 2, 4, 5, 6 and 10 are expressed on the cell surface and detect microorganismal components. Specifically, TLR 1, 2 and 6 detect lipoproteins (Kang et al., 2009), TLR4 responds to LPS (Janssen et al., 2011) and bacterial flagellin activates TLR5 (Hayashi et al., 2001). The function of TLR10 it yet unclear, however, it has been reported that TLR10 interacts with the HIV-1 gp41 protein (Henrick et al., 2019). The other types of TLRs are expressed intracellularly in endosomes (Rock, Hardiman, Timans, Kastelein, & Bazan, 1998), with TLR3 detecting double-stranded (ds) RNA (Alexopoulou, Holt, Medzhitov, & Flavell, 2001), TLR7 and 8

being activated by single stranded (ss) RNA (Diebold, Kaisho, Hemmi, Akira, & Reis e Sousa, 2004; Greulich et al., 2019) and TLR9 sensing unmethylated CpG-containing ssDNA (Hemmi et al., 2000).

1.3 Pyroptosis

Pyroptosis is one type of inflammasome-mediated programmed cell death that serves to avoid spread of intracellular pathogens like *Salmonella* spp., *Francisella* spp. and *Legionella* spp (Bergsbaken, Fink, & Cookson, 2009). Pyroptosis occurs mainly in infected macrophages, but also in other immune cell types and epithelial cells (Doitsh et al., 2014; Orzalli et al., 2021). Originally, pyroptosis was described as a caspase-1(cysteine-aspartic proteases-1) -dependent cell death of *Salmonella* infected cells (Hersh et al., 1999). After execution, pyroptosis leads to cell lysis and consequently to the release of pyrogenic cytokines, especially of the IL-1 family interleukins IL-1β and IL-18 (Kepp, Galluzzi, Zitvogel, & Kroemer, 2010), damage-associated molecular patterns (DAMPs) such as ATP, DNA, RNA and heat-shock proteins as well as the infection-inducing pathogen. This leads to recruitment and activation of other immune cells like neutrophils and uninfected macrophages, which on the one hand directly kill the pathogen (Miao et al., 2010) and on the other hand further drive inflammation and activate adaptive immunity (LaRock & Cookson, 2013).

The main features of pyroptosis are depicted in **Figure 1.1** and described in detail below. The induction and execution of pyroptosis is composed of a 3-step-process. ***Step 1***: priming signal, where LPS binds to TLR4 and activates NF-κB to induce transcription of pro-form proteins (pro-IL-1β, pro-IL-18, pro-caspase-1, pro-Gasdermin D) and inflammasome components. ***Step 2***: inflammasome activation by P2X7 receptor ligation with ATP, which opens ion channels. Thereby, efflux of potassium gives an assembly signal for the NLRP3 inflammasome, which in turn activates caspase-1 that cleaves pro-form proteins into their mature forms (IL-1β, IL-18, Gasdermin D). ***Step 3***: pyroptosis execution by gasdermin D translocation into the plasma membrane, which results in pore formation and thereby IL-1β, IL-18 release and water influx, resulting in cell swelling and rupture.

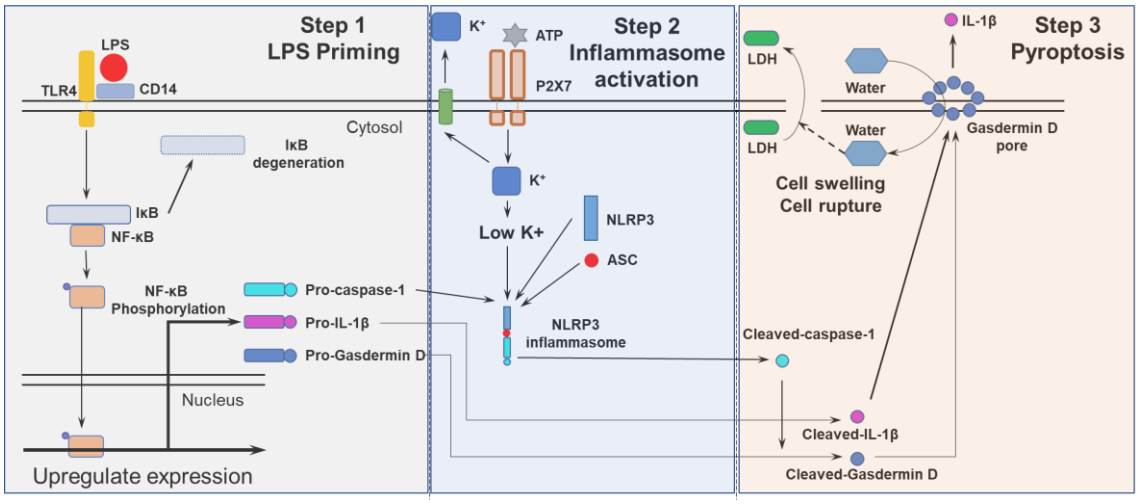

Figure 1.1 Principle of pyroptosis.

Step 1 LPS priming through TLR4 ligation and subsequent NF-κB activation, which leads to protein expression. ***Step 2 inflammasome activation*** by binding of ATP to P2X7 receptors which induces NLRP3 inflammasome assembly and caspase-1 activation. ***Step 3 pyroptosis execution*** where caspase-1 cleaves IL-1β and gasdermin D which results in pore formation and IL-1β release. Water influx causes cell swelling and cell membrane rupture.

1.3.1 Priming signal (1st signal of pyroptosis)

As mentioned in 1.3, induction of the pyroptotic process starts with a priming signal. In the case of LPS/ATP induced pyroptosis, LPS binding to CD14 and TLR4 triggers the activation of the myeloid differentiation primary response protein 88 (MyD88)-dependent signaling cascade. MyD88 recruits IL-1 receptor-associated kinase (IRAK) family members IRAK1 and IRAK4 in the cytosol, which subsequently activates tumor necrosis factor receptor-associated factor 6 (TRAF6) and transforming growth factor-β-activated protein kinase 1 (TAK1). A thereby formed TAK binding protein complex activates IκB kinase (IκK) which then phosphorylates the cytoplasmic NF-κB inhibitor IκB. Phosphorylated IκB dissociates from NF-κB, which then translocates into the nucleus to upregulate pro-caspase-1, pro-gasdermin D and pro-IL-1β expression as shown in Figure 1.2.

In addition to NF-κB, the TAK binding protein complex is also capable to activate the p38-MAPK signaling pathway which enhances pro-inflammatory cytokine production by AP-1 translocation into the nucleus. These pro-inflammatory pathways

are not only activated by TLR4, but also by TLR 2, 5, 7 and 9 (Gribar, Richardson, Sodhi, & Hackam, 2008).

Thus, the priming signal leads in macrophages to the production of components required for the inflammasome formation.

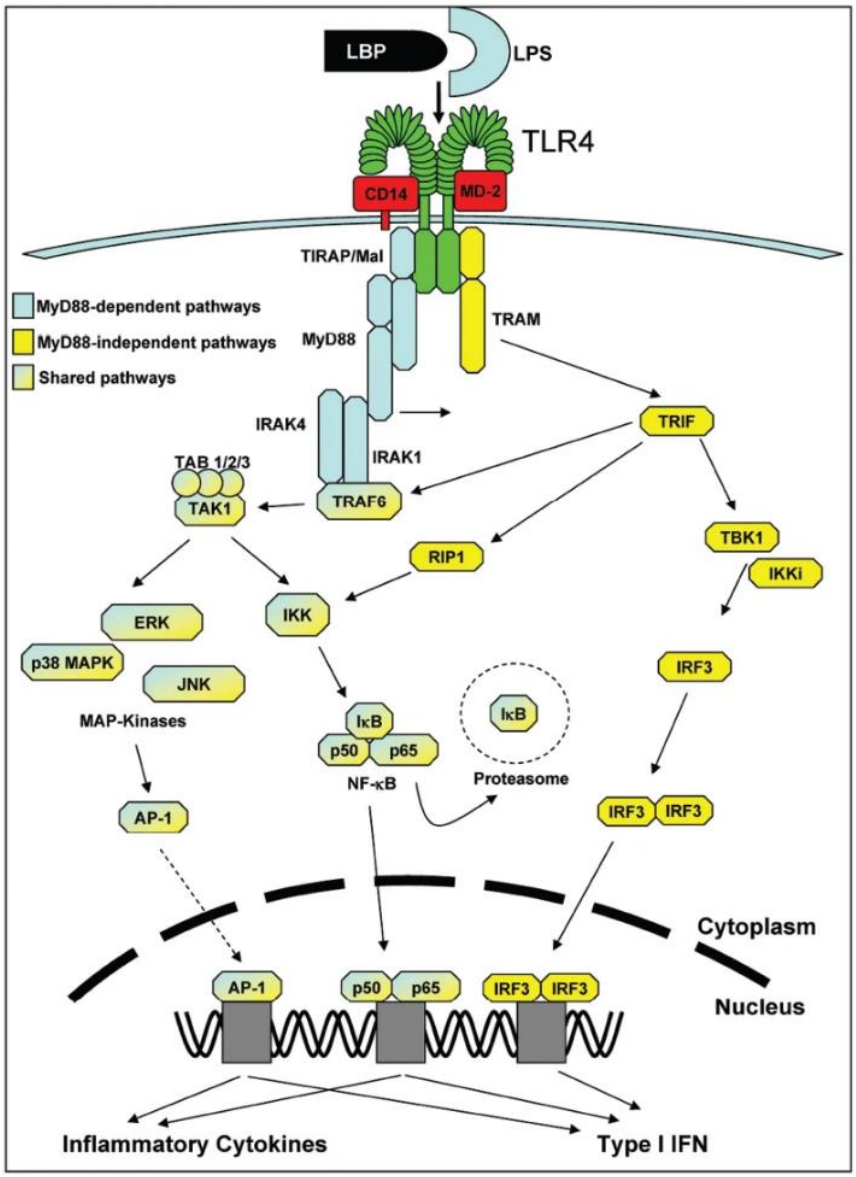

Figure 1.2 TLR4 signaling pathway.

TLR4 activation by LPS needs presence of CD14, MD2 and LPS binding protein (LBP). LPS bound TLR4 starts MyD88 dependent (blue) and independent (yellow) mechanisms to activate NF-κB, p38 MAPK or IRF signaling pathways for upregulation of inflammatory cytokines and Type I interferons (Gribar et al., 2008).

1.3.2 Inflammasome activation (2nd signal of pyroptosis)

An inflammasome is a multimeric complex consisting of NOD-like receptors (NLR) that sense danger signals, (pro-) caspase-1 that executes pyroptosis and apoptosis-associated speck-like protein (ASC) that links NLR and caspase-1 (Kesavardhana & Kanneganti, 2017). Dependent on the stimulus, different NLRs such as NLRP1, NLRP3, NLRC4, AIM2 and pyrin can be integrated into an inflammasome (Place & Kanneganti, 2018). The NLRP3 inflammasome is the most classical and best understood inflammasome. NLRP3 senses danger signals like extracellular ATP, pore-forming toxins, uric acid crystals and some pathogens (He, Hara, & Nunez, 2016). The distinct mechanism behind NLRP3 inflammasomes assembly is still under debate, but a recent study revealed a potassium efflux mechanism through TWIK2 (Di et al., 2018) to be responsible for NLRP3 inflammasome assembly.

The effector caspase-1 represents the first identified human caspase (Wilson et al., 1994). Originally, it was termed interleukin-1 converting enzyme (ICE) because of its function in cleaving pro-IL-1β into its mature form. After priming signal of pyroptosis, caspase-1 is expressed as pro-caspase-1 and it´s activated upon NLRP3 inflammasome assembly. The main cleavage targets of caspase-1 are not restricted to IL-1β and IL-18 (Netea et al., 2010). It also cleaves gasdermin D, the pore forming protein in pyroptosis, into its active form (X. Liu et al., 2016).

1.3.3 Execution phase of pyroptosis

After NLRP3 inflammasome assembly and proteolytical maturation of caspase-1, preformed pro-IL-1β, -IL-18 and -gasdermin D are cleaved into their active form. Unlike typical cytokines that contain N-terminal signal sequences for canonical endoplasmic reticulum/Golgi-mediated export, pro-IL-1β and -IL-18 reside in the cytosol until caspase-1-dependent release mechanisms are activated (Netea et al., 2010).

These two pro-inflammatory cytokines are strongly involved in inflammatory and autoimmune diseases like rheumatoid arthritis and Type I diabetes mellitus (Delaleu & Bickel, 2004). IL-1β is an endogenous pyrogen that induces fever, leucocyte recruitment and migration and release of other cytokines (Delaleu &

Bickel, 2004). IL-18 can trigger IFN-γ production for activation other immune cells (Nakanishi, Yoshimoto, Tsutsui, & Okamura, 2001).

Gasdermin D belongs to the pore-forming effector protein gasdermin family (Broz, Pelegrín, & Shao, 2020) and it is expressed in various human cells, especially in leukocytes and epithelial cells (Rieckmann et al., 2017). Activation of gasdermin D requires caspase-1- mediated cleavage of its linker region FLTD (Broz et al., 2020). Products of the cleavage are N-terminal gasdermin D (gasdermin D-NT; active domain) and C-terminal gasdermin D (repressor domain)(Shi et al., 2015). Active gasdermin D-NT fragments directly interact with phospholipids and form a pore on the cell membrane (Ding et al., 2016) which allows IL-1β and IL-18 release (Fink & Cookson, 2006).

This non-selective pore allows a passage of water and ions causing cell swelling and ultimately cell membrane rupture and cell lysis, which results in the release of intracellular contents such as lactate dehydrogenase (LDH), a quantification marker of pyroptosis induction. Additionally, DAMPs released by pyroptotic cells recruit and activate nearby primed cells causing chronic, prolonged inflammation (Galluzzi et al., 2018; LaRock & Cookson, 2013).

However, cell lysis is not the only consequence of gasdermin D pore formation. Hyperactive macrophages release IL-1β and IL-18 through gasdermin D pore without detectable cell lysis (Evavold et al., 2018). The gasdermin D pore has a diameter of 10-15 nm (Sborgi et al., 2016). This allows a release of small molecules like cytokines (diameter of 4.5 nm) in the extracellular space, but not of large molecules such as LDH (diameter of 25 nm).

Altogether, pyroptosis serves to fight against pathogenic infection by macrophages and to limit spread of infection but it may also induce severe inflammation.

1.4 Glucocorticoids as regulators of inflammation

Glucocorticoids (GCs) are adrenal hormones which are released in response to stress. The GC cortisol is synthesized and secreted in the cortex of human adrenal glands and regulated by the hypothalamic-pituitary-adrenal (HPA) axis (Rhen & Cidlowski, 2005). Most of the cortisol is bound to corticosteroid-binding

globulins in blood (Breuner & Orchinik, 2002). The remaining unbound corticol exerts biological activity (S. Yang & Zhang, 2004).

Cortisol or Hydrocortisone (HC) is a lipophilic hormone, which spontaneously diffuses trough the membrane and binds to its cytoplasmic glucocorticoid receptor (GR). GRs are constitutively expressed in all nucleated cells (Cain & Cidlowski, 2017). Once bound and activated by GCs, GR translocates into the nucleus and interacts with DNA, to either enhance or repress gene expression by one of the three mechanisms of genomic effects: 1) direct binding to glucocorticoid-responsive elements (GREs) of a gene promoter; 2) tethering to other transcription factors (TFs) like NF-κB, which indirectly interacts with DNA; 3) direct binding to DNA and interaction with nearby TFs (e.g. AP-1), which is known as composition (Cruz-Topete & Cidlowski, 2015). In addition to genomic effects, GRs can interact with phosphokinases for rapid non-genomic effects within minutes (Boldizsar et al., 2010). The detailed mechanisms of non-genomic effects are still under investigation. However an involvement in immune system responses was described (Ayroldi et al., 2012).

GCs are important regulators of inflammation. Natural GCs such as cortisol and synthetically produced HC are widely used in clinical practice as anti-inflammatory drugs. The anti-inflammatory activity of cortisol/HC and other GCs is mainly attributed to the suppressed gene expression of pro-inflammatory cytokines (e.g., IL-1β, IL-6, TNF) and adhesion molecules (e.g., ECAM-1, ICAM-1) by direct interaction with GREs (Cronstein, Kimmel, Levin, Martiniuk, & Weissmann, 1992). Moreover, these hormones inhibit NF-κB, p38-MAPK and other signaling pathways related to pro-inflammatory immune responses. Inhibiting these pathways suppress leukocyte chemotaxis, migration, differentiation and activation (Franchimont et al., 2000; Piemonti et al., 1999) and consequently inflammation. Observation studies on human adrenalectomy or adrenal insufficiency which leads to lack of GCs production showed enhanced immune responses like increased phagocytosis by macrophages and pro-inflammatory cytokine production (Bishayi & Ghosh, 2007; Rahvar, Riesel, Graf, & Harbeck, 2019). However, the capability of killing pathogens was impaired (Bishayi, Ghosh, & Bhanja, 2003), which in turn illustrates the function of HC/GCs in reducing inflammation and regulating pathogen clearance.

Apart from the described anti-inflammatory effects, GCs display unexpected pro-inflammatory or immune-sensitizing properties. Low-dose GC treatment of LPS/IFN-γ activated macrophages for instance induced gene expression of pro-inflammatory cytokines, including IL-1β, IL-6, IL-12, CXCL1, CXCL10 and TNF (Lim, Müller, Herold, van den Brandt, & Reichardt, 2007). A genome-wide expression study on peripheral blood mononuclear cells (PBMCs) showed that TLR2, TLR4, NLRP3, and purine receptor PY2R2 are promoted by low-dose GCs (Busillo & Cidlowski, 2013), and downstream of the receptors are pro-inflammatory cytokines like IL-1β, IL-6 and TNF. These findings suggest that low-dose GCs sensitize innate immune cells for rapid responses.

Altogether, GCs act both as pro- and anti-inflammatory hormones. To understand how and in which condition GCs and HC in special regulate immune responses will provide insight into its directed application.

1.5 Aim of research

Pyroptosis of macrophages, which is induced by pathogen infection, leads to the release of pro-inflammatory cytokines such as IL-1β and may result in severe inflammation. HC is commonly used as therapeutic against inflammatory diseases. This is based on the general ability of HC to modulate inflammation by regulating involved signaling pathways or by the enhancement of extracellular receptor expression. However, by now it was not distinguished between the effects of HC when administred at two different conditions: 1) when HC is administred to improve an inflammation state which is caused by infection (acute) or 2) when infection occurs under constantly high cortisol/HC concentrations like in very stressed persons or patients under continuous HC treatment (chronic).

The aim of this study was to investigate, if an acute or chronic administration of high HC doses differentially influences pyroptosis. For this purpose, pyroptosis was induced *in vitro* in a THP-1 macrophage-like cell line under either acute or chronic HC co-incubation and essential steps and phases of pyroptosis were investigated, namely the *priming* phase, *inflammasome activation* phase and *execution* phase.

These results may contribute to the identication of different effects of HC on macrophages in inflammation and direct to the importance of considering IL-1β as a standard inflammation marker in the clinical routine.

2. Material and Methods

2.1 Materials

Lists below are materials used in this study.

2.1.1 Instruments

Table 2.1 Instrument list

Instrument	Company	Type
Cell counter	Bio-Rad	TC20
Centrifuge	Thermo Scientific	Heraeus 40R
Clean Bench	Heraeus	HS 12/2
CO_2 Incubator	Binder	CB 220
Developer system	Agfa	CURIX 60
Flow cytometer	Beckton Dickinson	FACScan
Flow cytometer	Merck Millipore	Guava 8HT
Gel Casting Stand	Bio-Rad	Mini-PROTEAN® Tetra
Laser Scanning Confocal Microscope	Leica	SP5 II
Microcentrifuge	Eppendorf	5430R
Microplate Reader	Molecular Devices	EMax Plus
Microscope with camera	Leica	DMiIL
Microvolume Spectrophotometer	Thermo Scientific	NanoDrop One
Mini Trans-Blot® Module	Bio-Rad	Mini-PROTEAN® Tetra
Power Supply	Bio-Rad	PowerPac™ Basic
Real-Time PCR Systems	Applied Biosystems	StepOnePlus
Thermal cycler	Applied Biosystems	GeneAmp 2700
Thermal mixer	Eppendorf	Thermomixer C
Ultra-Low Freezer	Eppendorf	F740i
Vertical Electrophoresis Cell	Bio-Rad	Mini-PROTEAN® Tetra

2.1.2 Reagents and Chemicals

Table 2.2 List of reagents and chemicals

Reagent	Company	Catalog Number
2-Propanol	Merck	1.09634.1011
37% Formaldehyde	Carl Roth	4979.1
4',6-diamidino-2-phenylindole	Sigma-Aldrich	A9542
Accutase	Invitrogen	00-4555-56
Acrylamide/Bis acrylamide 37.5:1 (30%)	Sigma-Aldrich	A3699
Adenosine 5'-triphosphate disodium salt hydrate	Sigma-Aldrich	A6419
Ammonium Persulfate	Sigma-Aldrich	A3678
Bovine Serum Albumin	Carl Roth	8076.4
Dimethyl sulfoxide	Sigma-Aldrich	RNBH3501
Dithiothreitol	Sigma-Aldrich	43815
Ethanol	Merck	1.08543
Glycerol	Carl Roth	3787
Glycine	Sigma-Aldrich	G8898
Hydrochloric acid	Merck	1.09063
Hydrocortisone	Pfizer	-
Lipopolysaccharide from E.Coil O26:B6	Sigma-Aldrich	L2654
Methanol	Sigma-Aldrich	32212
N,N,N',N'-Tetramethylethylenediamine	Bio-Rad	161-800
Non-fat milk powder	Bio-Rad	170-6404
Phorbal 12-myristate 13-acetate	Sigma-Aldrich	P1585
Poly-L-lysine	Sigma-Aldrich	P4832
Protein A agarose beads	CST	9863
Protein Ladder	Invitrogen	26616
Sodium Dodecyl Sulfonate	Sigma-Aldrich	L3771
Tris	Merck	1.08382
Triton X-100	Sigma-Aldrich	T6878
Tween 20	Sigma-Aldrich	P7949
Vectashield	Vector Laboratories	H-1000

2.1.3 Consumables

Table 2.3 List of consumables

Product	Company	Catalog Number
0.2 ml Microcentrifuge tube RNase free	Sarstedt	72.737
1.5 ml Microcentrifuge tube	Sarstedt	72.706
1.5 ml Microcentrifuge tube RNase free	Sarstedt	72.706.200
1.8 ml Cryopreservation tube	Nunc	363401
15 ml Centrifuge tube	Sarstedt	02.554.002
50 ml Centrifuge tube	Sarstedt	02.559.001
10 µl pipette tip	Eppendorf	0030.000.811
200 µl pipette tip	Eppendorf	0030.000.889
1000 µl pipette tip	Sarstedt	70.3050.020
20 µl pipette tip RNase free	Sarstedt	70.1114.210
200 µl pipette tip RNase free	Sarstedt	70.3031.255
1000 µl pipette tip RNase free	Sarstedt	70.3050.255
T25 cell culture flask	Greiner Bio-One	690175
T75 cell culture flask	Greiner Bio-One	658175
96-well plate	Falcon	351172
12-well plate	Greiner Bio-One	665184
6-well plate	Greiner Bio-One	657164
5 ml Serological pipette	Sarstedt	86.1253.001
10 ml Serological pipette	Sarstedt	86.1254.001
25 ml Serological pipette	Sarstedt	86.1685.001
12X75 mm reaction tube	Falcon	352053
0.4µm Nitrocellulose Membrane	Bio-rad	162-0145
Cover slide	MARIENFELD	0117580
Microscope slide	Thermofisher	J1800AMNZ

2.1.4 Commercial test kits

Table 2.4 List of commercial test kits

Product	Company	Catalog Number
Cytofix/Cytoperm™ Fixation/Permeabilization Kit	BD Bioscience	554714
CytoTox 96® Non-Radioactive Cytotoxicity Assay	Promega	G1780
ECL Primer Western Blotting detection reagents	GE healthcare	RPN2232
FLICA-YVAD-FMK	Immunochemistry	9145
Human Caspase-1 ELISA Kit	Thermo Scientific	EH70RB
Human IL-1β ELISA kit	Invitrogen	KAC1211
Maxima™ H Minus cDNA SynthesisMaster Mix	Thermo Scientific	M1661
Nucleospin RNA Kit	MACHEREY-NAGEL	740955
Pierce BCA Protein Assay Kit	Thermo Scientific	23225
PowerUP SYBR® Green PCR Master Mix	Applied Biosystems	A25741
SuperSignal West Dura Substrate	Thermo Scientific	34075

2.1.5 Cell line

Table 2.5 Cell line

Product	Provider	Catalog Number
THP-1	ATCC	TIB-303

2.1.6 Cell Culture Medium

Table 2.6 Cell Culture Medium

Product	Company	Catalog Number
RPMI-1640	Gibco	21875-034
RPMI-1640 without Phenolred	Gibco	11835-063
Fetal Bovine Serum	PAN biotech	P30-8500
Penicillin-Streptomycin	PAN biotech	P06-07050

Complete cell culture medium: 445 ml RPMI-1640 + 50 ml FBS (10% v/v) + 5ml P/S (1% v/v)

Pyroptosis induction medium: 470 ml RPMI-1640 without Phenolred + 25 ml FBS (10% v/v) + 5ml P/S (1% v/v)

2.1.7 Antibodies

Table 2.7 Antibody list for Western Blot

Target	Company	Catalog number	Label	Clone	Origin	Dilution	Dilution Buffer
Primary Antibodies							
ASC/TMS1	CST	13833	-	E1E3I	Rabbit	1 : 1000	5% BSA
Caspase-1	CST	3866	-	D7F10	Rabbit	1 : 1000	5% BSA
Caspase-1 cleaved	CST	4199	-	D57A2	Rabbit	1 : 1000	5% BSA
GAPDH	CST	5174	-	D16H11	Rabbit	1 : 10000	5% milk
Gasdermin D	CST	96458	-	-	Rabbit	1 : 1000	5% BSA
IL-1β	CST	12703	-	D3U3E	Rabbit	1 : 1000	5% BSA
IL-1β cleaved	CST	83186	-	D3A3Z	Rabbit	1 : 1000	5% BSA
NF-κB p65	CST	8242	-	D14E12	Rabbit	1 : 1000	5% BSA
NF-κB p65 pSer^{562}	CST	3033	-	93H1	Rabbit	1 : 1000	5% BSA
NLRP3	CST	15101	-	D4D8T	Rabbit	1 : 1000	5% BSA
NLRP3	AdipoGen	AG-20B-0014	-	Cryo-2	Mouse	1 : 200	5% BSA
β-Actin	CST	4967	-	-	Rabbit	1 : 5000	5% BSA
Secondary Antibodies							
Anti-Rabbit IgG	CST	7074	HRP	-	Goat	1 : 2500	5% BSA
Anti-Mouse IgG	CST	7076	HRP	-	Horse	1 : 2500	5% BSA

Table 2.8 Antibody list for Immunocytochemistry

Target	Company	Catalog number	Label	Clone	Origin	Dilution	Dilution Buffer
Primary Antibodies							
ASC/TMS1	CST	13833	-	E1E3I	Rabbit	1 : 100	2% BSA
NF-κB p65	CST	8242	-	D14E12	Rabbit	1 : 400	2% BSA
NLRP3	AdipoGen	AG-20B-0014	-	Cryo-2	Mouse	1 : 400	2% BSA
Secondary Antibodies							
Anti-Rabbit IgG	Invitrogen	F2765	FITC		Goat	1 :500	2% BSA
Anti-Mouse IgG	Invitrogen	A11030	Alexa-Fluor546		Goat	1 : 500	2% BSA

Table 2.9 Antibody list for Flow cytometry

Target	Company	Catalog number	Label	Clone	Origin	Amount	Staining Buffer
IL-1β	Biolegend	511705	FITC	H1B-96	Mouse	0.5 μg/test	PBS
CD11b	Miltenyi	130-113-231	APC	M1/70	Mouse	0.5 μg/test	PBS

2.1.8 Synthetic nucleotides

Table 2.10 Sequences of Primers for qPCR

IL-1β forward primer	5'-TTACAGTGGCAATGAGGATGAC-3'
IL-1β reverse primer	5'-GTCGGAGATTCGTAGCTGGAT-3'
18S rRNA forward primer	5'-GGACAGGATTGACAGATTGATAG-3'
18S rRNA reverse primer	5'-CTCGTTCGTTATCGGAATTAAC-3'

Lyophilized primers were reconstituted with RNase-free H_2O to 100 pmol/μl, then diluted 1:20 with RNase-free H_2O to make PrimerMix as follows:

IL-1β PrimerMix	Forward 10 μl (1 nmol) Reverser 10 μl (1 nmol) H_2O 180 μl	18S rRNA PrimerMix	Forward 10 μl (1 nmol) Reverse 10 μl (1 nmol) H_2O 180 μl
Total	200 μl (5 μM for each primer)	Total	200 μl (5 μM for each primer)

PrimerMixes were stored at -20 °C.

2.1.9 Buffers and Solutions

Table 2.11 Buffers and solutions for cell culture

Composition	Provider	Quantity	Catalog Number
PBS 500 ml			
NaCl	Apotheke, Klinikum der Universität München	4.0 g	APO-ST016
KCl		0.1 g	
$Na_2HPO_4 \cdot 2H_2O$		0.575 g	
KH_2PO_4		0.1 g	
H_2O		To 500 ml	
Cell Freezing Medium 2 ml			
Fetal Bovine Serum	PAN biotech	1 ml	
DMSO	Sigma-Aldrich	1 ml	

Table 2.12 Buffers and Solutions for Western Blot

Composition	Provider	Quantity	Catalog Number
Cell lysis buffer 1 ml			
Cell Lysis Buffer (10 ×)	CST	100 µl	9803
Halt™ Protease and Phosphatase Inhibitor Cocktail (100 ×)	Thermo Scientific	10 µl cocktail 10 µl EDTA	78442
H_2O		880 µl	
Tris 1 M pH 6.8 50ml			
Tris	Merck	6.057 g	1.08382
HCl	Merck	to pH 6.8	1.09063
ddH_2O	-	to 50 ml	
Tris 1.5 M pH 8.8 50ml			
Tris	Merck	9.067 g	1.08382
HCl	Merck	to pH 8.8	1.09063
ddH_2O	-	to 50 ml	
6× Laemmli Buffer 8 ml			
SDS	Sigma-Aldrich	1.2 g	L3771
Bromophenol blue	Bio-Rad	6 mg	161-0404
Glycerol	Roth	4.7 ml	3783
Tris 1M pH 6.8	-	1.2 ml	-
DTT	Sigma-Aldrich	0.93 g	43815
ddH_2O	-	2.1 ml	-
Blue Loading Buffer 1 ml			
3× Blue Loading Buffer	CST	900 µl	7722
30× Reducing Agent (1.25 M DTT)		100 µl	
SDS Running Buffer 1000 ml			
Tris	Merck	3.02 g (25 mM)	1.08382
Glycine	Sigma-Aldrich	14.41 g (192 mM)	G8898
SDS	Sigma-Aldrich	1 g	L3771
HCl	Merck	to pH 8.3	1.09063
ddH_2O	-	to 1000 ml	
Transfer Buffer 1000 ml			
Tris	Merck	3.02 g (25 mM)	1.08382
Glycine	Sigma-Aldrich	14.41 g (192 mM)	G8898
Methanol	Sigma-Aldrich	200 ml	32212
ddH_2O	-	to 1000 ml	-
TBS-T 500 ml			
TBS pre-mixed powder	Biozym	1 bag	541049
ddH_2O	-	To 500 ml	
Tween 20	Sigma-Aldrich	500 µl	P7949
5% BSA 100ml			
Bovine Serum albumin	Roth	5 g	8076.4
TBS-T	-	to 100 ml	-
5% No-fat milk			
No-fat milk powder	Bio-Rad	5 g	170-6404
TBS-T	-	to 100 ml	

Table 2.13 Preparation of separation gel and stacking gel for SDS-PAGE

Separation Gel	12%	10%	7.5%
ddH_2O	6.67ml	8ml	9.67ml
Tris-HCl (1.5M pH8.8)	5ml	5ml	5ml
Acrylamide/Bis acrylamide (30%)	8ml	6.67ml	5ml
10% SDS	200µl	200µl	200µl
10% APS	100µl	100µl	100µl
TEMED	30µl	30µl	30µl
Total Volume	20ml	20ml	20ml

Stacking Gel	5%
ddH_2O	5.502ml
Tris-HCl (1.0M pH6.8)	1ml
Acrylamide/Bis acrylamide (30%)	1.33ml
10% SDS	80µl
10% APS	80µl
TEMED	8µl
Total Volume	8ml

Table 2.14 Buffers and Solutions for Immunocytochemistry

Composition	Provider	Quantity	Catalog Number
2% Fixation Buffer 10 ml			
37% Formaldehyde	Roth	0.55 ml	4979.1
PBS	Apotheke, Klinikum der Universität München	9.45 ml	APO-ST016
0.5% Permeabilization Buffer 10ml			
Triton X-100	Sigma-Aldrich	50 µl	T6878
PBS	Apotheke, Klinikum der Universität München	10 ml	
PBS-T 500ml			
PBS	Apotheke, Klinikum der Universität München	500 ml	
Tween 20	Sigma-Aldrich	500 µl	P7949
2% BSA 10ml			
Bovine Serum albumin	Roth	2 g	8076.4
PBS-T		100 ml	

2.1.10 Softwares for analysis

Table 2.15 Software list

Product	Provider	Version
ImageJ	NIH	1.53
LAS X	Leica	-
SPSS	IBM	26.0
SoftMax	Molecular Devices	7.0
GraphPad Prism	GraphPad Software	9.01
CellQuest Pro	BD	
InCyte	Merck	3.0

2.2 Methods

2.2.1 Cell Culture

2.2.1.1 Cultivation

THP-1 cells were cultivated in suspension in T75 flasks at 37 °C and 5% CO_2 in a humidified atmosphere. When reaching a density more than 1×10^6 /ml, cells were collected, centrifuged (300 x g, 5 min) and resuspended in fresh cell culture medium in a density of 5×10^5 /ml. Doubling time for THP-1 cells was approximately 48 hours. Cells were harvested at density of 1×10^6 /ml for THP-1 macrophage-like cell induction.

2.2.1.2 Cryoconservation and thawing

Cells were frozen at a density of 3×10^6 /ml in RPMI-1640 complete cell culture medium and an equal volume of cell freezing medium. 1.8 ml cryogenic tubes (Nunc) were placed into a Mr. Frosty™ Freezing Container (Thermo Fisher) and frozen at -80 °C. After 24 hours at -80 °C, cells were transferred to liquid nitrogen vapor phase for long time cryopreservation.

Frozen cells were thawed in 37 °C water bath and transferred to 10 ml prewarmed complete cell culture medium. The cell suspension was centrifuged (300 × g, 5 min), supernatant was discarded to remove DMSO and cell pellet was resuspended in fresh complete cell culture medium at the density of 5×10^5 /ml for further cultivation.

2.2.1.3 THP-1 cells differentiation into macrophage-like cells

For pyroptosis experiments, THP-1 cells were differentiated into macrophage-like cells. For determination of the most efficient condition for differentiation, 0-500 ng/ml PMA was added to cell suspension at a density of 1×10^6 cells/ml (Table 2.16), and afterwards cells were seeded into multi-well plates (for 6 well-plate in 2 ml, for 12 well-plate in 1 ml), and incubated at 37 °C, 5% CO_2 for 0-72 hours. Then, PMA-containing medium was discarded, cells were washed twice with prewarmed PBS and incubated in fresh cell culture medium for 24 hours until pyroptosis induction.

Table 2.16 PMA duration and concentration optimization.

PMA treatment duration (concentration 100 ng/ml)	PMA concentration (treatment for 48 hours)
0h	0 ng/ml
2h	5 ng/ml
4h	10 ng/ml
8h	25 ng/ml
24h	50 ng/ml
32h	100 ng/ml
48h	250 ng/ml
72h	500 ng/ml

2.2.1.4 Pyroptosis induction and hydrocortisone treatment

For optimization of pyroptosis induction, THP-1 macrophage-like cells were washed twice with pre-warmed PBS and taken up in pyroptosis induction medium, containing LPS (0-100 ng/ml or as indicated) for 1 or 3 hours for cell priming. Thereafter ATP was added to a final concentration of 0-10mM. After ATP treatment for 0.5-3 hours (Table 2.17-2.18), supernatants and cell pellets were collected for further analysis.

For HC treatment, THP-1 macrophage-like cells were incubated with 0-0.4 µg/ml HC 24 hours prior to LPS priming (PreLPS). After HC pre-incubation, cell culture medium was replaced with fresh medium containing 5 ng/ml LPS and HC (0 - 0.4 µg/ml) (PostLPS) according to different conditions. Chronic HC included 0.2 or 0.4 µg/ml Pre- and PostLPS, acute HC comprised 0.1 µg/ml HC PreLPS followed by 0.2 or 0.4 µg/ml HC PostLPS. One hour after LPS priming, 5 mM ATP was added to induce inflammasome activation. In total, cells were harvested 3.5 hours after priming for downstream analysis.

Table 2.17 LPS and ATP concentration optimization.

LPS concentration (ATP 5mM)	ATP concentration (LPS 5ng/ml)
0 ng/ml	0 µM
5 ng/ml	100 µM
10 ng/ml	500 µM
50 ng/ml	1 mM
100 ng/ml	5 mM
	10 mM

Table 2.18 LPS and ATP treatment duration optimization.

LPS duration (ATP 5mM)	ATP concentration (LPS 5ng/ml)
1 h	0.5 h
3 h	1 h
	1.5 h
	2 h
	2.5h
	3 h

2.2.2 Cytotoxicitiy measurements by Lactate Dehydrogenase assay

After pyroptosis induction with/without acute or chronic HC exposure, cell culture supernatants were collected and centrifuged (500 × g, 5 min) to remove debris. 50 µl clear supernatant was transferred into a 96-well plate. LDH release was measured by CytoTox 96® Non-Radioactive Cytotoxicity Assay. For this, 50 µl assay buffer were added into each well and the plate was incubated in the dark at room temperature for 30 min. LDH, which is released from damaged cells oxidizes lactate and provides NADH. In presence of diaphorase, NADH converses iodonitrotetrazolium violet (INT) into red formazan. The intensity of red color reflects the amount of released LDH released. The reaction was stopped by adding 50 µl stop solution into the wells. Optical Density (O.D.) at 490 nm was measured by a microplate reader.

2.2.3 Protein-chemical methods

2.2.3.1 Interleukin-1β and Caspase-1 quantification by Enzyme-Linked Immunosorbent Assay (ELISA)

Human IL-1β or caspase-1 concentrations in cell culture supernatants were measured by *Human IL-1β ELISA kit* or *Human Caspase-1 sandwich ELISA Kit*, respectively. Cell culture supernatant was transfered into capture antibody pre-coated wells and incubated according to manufacturers instructions. After incubation, wells were washed to remove unbound antigen. Biotinylated detection antibody was then added and incubated according to manufacturers instructions. Wells were washed again to remove unbound detection antibody. Streptavidin-Horseradish peroxidase (HRP) solution was added and incubated according to manufacturers instructions. Finally, protein detection was performed with the HRP substrate 3,3',5,5'-Tetramethylbenzidine (TMB) and terminated by stop solution. Optical Density (O.D.) was read by microplate reader at 450nm. Standard curve was fitted by 4-parameter algorithm by SoftMax Pro 7.0.

2.2.3.2 Protein extraction for Western Blot and Co-immunoprecipitation

Cells were harvested and centrifuged together with respective supernatants to obtain also detached or dying cells. After washing with cold PBS, cells were re-suspended in cell lysis buffer adjusted to the cell number (100 µL buffer for $1x10^6$ cells) and incubated on ice for 20 min. Cell lysates were sonicated (3 seconds at 50% power, output 3) and centrifuged (14,000 × g, 10 min, 4 °C). Protein-containing supernatants were collected for protein quantification and subsequently processed for further analysis.

2.2.3.3 Protein quantification

Protein amount in the cell lysate was determined by Pierce BCA Protein Assay Kit in accordance with the manufacturers protocol. O.D. was read by a microplate reader at 562 nm. Standard curve was linear fitted by SoftMax Pro 7.0. Protein lysate was then diluted to 1.0 µg/µl with cell lysis buffer.

2.2.3.4 Co-Immuno-precipitation (Co-IP)

1 µl mouse anti-NLRP3 antibody was added to 200 µg cell lysate and incubated on the tube roller at 4 °C overnight. The next day, 20 µl protein A agarose beads were added into the tube and incubated for further 4 hours for the conjugation of protein A and antibody. Protein-antibody-beads complex were washed five times with cell lysis buffer, and then resuspended with 20 µl of 3 × Blue loading buffer and heated at 95 °C for 5 min for protein denaturation. Samples were spinned down and stored at -80 °C.

2.2.3.5 Preparation of protein extracts for SDS-PAGE

Protein samples were mixed with 6 × Laemmli Buffer. To enable access of antibody to the epitope proteins were denaturated at 95 °C for 5 min. Samples were spinned down and stored at -80 °C.

2.2.3.6 Sodium Dodecyl Sulfate Polyacrylamide Gel Electrophoresis (SDS-PAGE)

SDS-Gels were installed into Mini-PROTEAN Tetra Vertical Electrophoresis Cell, and filled with SDS-PAGE Running Buffer. Combs were carefully removed, 20 µl (20 µg) of sample was loaded into wells, 10 µl of protein ladder was loaded as molecular weight standard. In empty wells 20 µl of 1 × loading buffer was loaded to avoid shifting of the band.

Electrophoresis program was set at 80 V for 5 min followed by 100 V for 70 min until bromophenol blue ran to the bottom of the gel.

2.2.3.7 Western Blot -Transfer on Nitrocellulose membranes

After SDS-PAGE, gel was carefully removed from glass plates and soaked in transfer buffer to wash away residual running buffer. The *Transfer Sandwich* was prepared in the transfer buffer as follows: sponge, 2x Whatman paper, NC-membrane, SDS-gel, 2x Whatman paper, sponge. Blotting time in transfer buffer was 90 min at constant 80 V under continuous cooling.

2.2.3.8 Antibody incubation and protein detection on nitrocellulose membranes

After western blotting, membranes were washed with TBS-T and blocked with 5 % non-fat dry milk for one hour at room temperture under gentle shaking. After blocking, membranes were incubated with primary antibodies with dilutions as listed in Table 2.7 at 4 °C overnight. Then, membranes were washed three times with TBS-T and incubated with secondary antibodies for one hour at room temperature. After incubation, membranes were washed three times with TBS-T and proteins were visualized with the detection reagent SuperSignal West Dura Substrate on X-ray films.

X-ray films with bands were scanned and analyzed by ImageJ software, gray-scale value of band was measured and normalized to β-actin or GAPDH.

2.2.4 Immunocytochemical staining

2.2.4.1 Preparation of cells on cover slide

Autocleaved 18 mm diameter coverslips were inserted into a 12-well plate and covered with 300 µl poly-L-lysine (37 °C, 1 hour) to prevent cell detachment after pyroptosis induction. Subsequently, excess poly-L-lysine was removed and coverslips were dried under the clean bench. Afterwards, $1x10^6$ cells were seeded in 1 ml cell culture medium and differentiation and pyroptosis was induced as indicated in 2.2.1.

2.2.4.2 Antibody staining

Cells were washed three times with pre-warmed PBS and fixed with 2 % fixation buffer for 10 min. Then cells were washed twice with PBS-T and permeabilized with 0.5 % Triton X-100/PBS for 10 min. After three times stepwise washing with PBS-T, cells were blocked with 1 ml 2 % BSA/PBS-T for 10 min.

Incubation with primary antibodies was performed for one hour in dilutions as indicated in Table 2.8. Afterwards, coverslips were washed three times with PBS-T and incubated for one hour with the respective fluorophore-conjugated secondary antibodies. For both antibody incubation steps it is essential to keep the coverslips in a humid dark incubation chamber to avoid fading and drying out.

After antibody incubation, cells were washed three times with PBS-T and post-fixated for 10 min with 2 % fixation buffer in the dark and DNA was counterstained for 10 min with DAPI (20 µg/ml). After a last washing step with ddH_2O, cells on coverslips were mounted with one drop of Vectashield mounting medium on the microscope slides and then edges were sealed with nail polish.

All steps were performed at room temperature.

2.2.4.3 Confocal Microscopy and data analysis

For detection of the antigens that were stained with fluorochrome-conjugated antibodies, slides were analyzed by Laser Scanning Confocal Microscope with a 63X objective and oil immersion. For excitation of DAPI, 405 nm laser was used, for FITC, the 488 nm laser, and for AlexaFluor 546 the 561 nm lasers were used. Filters for DAPI, FITC and TRITC were selected to receive signal. Images were acquired with LAS X software and analyzed with ImageJ software (developed at the National Institutes of Health and not subject to copyright protection).

2.2.5 Flow cytometry

2.2.5.1 Staining of cell surface CD11b

THP-1 macrophage-like cells were detached with accutase and washed with PBS. For CD11b staining, 100,000 cells/well were transferred into a 96-well plate and incubated with 5 µl APC-anti-human-CD11b antibody (20 min, room temperature, in the dark). Afterwards, cells were washed twice with PBS and resuspended in 200 µl PBS for measurement. Percentage of CD11b positive cells was measured by Guava 8HT flow cytometer (red laser) and analysed by InCyte Software.

2.2.5.2 Intracellular Interleukin-1β staining

THP-1 macrophage-like cells were detached with accutase and washed with pre-warmed PBS. Intracellular staining was performed with BD Cytofix/Cytoperm™ Fixation/Permeabilization Kit according to manufacturers instructions. Briefly, cells were resuspended in 250 µl Fixation/Permeabilization solution and incubated at 4 °C for 20 min. Subsequently cells were washed twice with 1 ml 1× BD Perm/Wash™ buffer and then resuspended in 50 µl of the same buffer. 5 µl (0.5

µg) FITC-anti-human-IL-1β antibody was added and incubated for 30 min at 4 °C in the dark. After an additional washing step with 1× BD Perm/Wash™ buffer, cells were resuspended in 300 µl PBS. The mean fluorescence index (MFI) of intracellular IL-1β was measured by FASCan flow cytometer (blue laser, FL-1 channel) and analyzed by BD CellQuest Pro.

2.2.5.3 Staining of pyroptotic cells with caspase-1 tracker and propidium iodide

After pyroptosis induction, THP-1 macropahges were washed three times with pre-warmed PBS and incubated in 300 µl PBS containing 1 × caspase-1 tracker FLICA-YVAD-FMK for one hour at 37 °C with swirling cells every 20 min. Subsequently, cells were washed twice with 2 ml 1X Cellular Wash Buffer and stained with 0.5 % (v/v) Propidium Iodide (PI)/PBS (500 µl) for 5 min in the dark at room temperature to detect cells with broken membrane/dead cells. After two washing steps with PBS and cell detachment with accutase, cells were resuspended with 300 µl PBS and percentage of pyroptotic cells was assessed by FASCan flow cytometer (blue laser). FAM-FLICA was detected by FL-1 and PI was detected by FL-3. FAM-FLICA$^+$ PI$^+$ cells were regarded as pyroptotic cells.

2.2.6 Quantitative Reverse Transcription Polymerase Chain Reaction (qRT-PCR) for detection of IL-1β mRNA

2.2.6.1 RNA extraction and quantification

1x10^6 cells were harvested and washed with PBS. Cellular RNA was isolated using Nucleospin RNA Kit. Cell pellets were lysed in 350 µl RA1 buffer supplemented with 1% β-mercaptoethanol, then added in the filtration column for centrifugation at 11,000 g for 1 min. Flowthrough was collected and mixed with 350 µl 70 % ethanol. RNA was bound on a column by centrifugation at 11,000 g for 30 seconds. After RNA binding, column was desalted with MDB buffer, followed by DNA digestion with rDNase for 15 min. After this step, the column was washed to inactivate DNase and purify RNA which was finally eluted with 60 µl RNase-free water by centrifugation at 11,000 g for 1 min.

RNA concentration was determined by Nanodrop One. The ratio of the absorbance at 260/280 nm (A260/A280) and 260/230nm (A260/A230) was measured to determine the RNA purity. Good RNA quality had A260/A280 and A260/230 ratio of ~2.0. RNA samples were diluted to 62.5 ng/µl with RNase-free H_2O. Samples were stored at -80 °C.

2.2.6.2 Reverse Transcription to obtain cDNA

16 µl sample containing 1 µg RNA or water (as non-template control) was transferred into a 0.2 ml PCR tube, and heated to 65 °C for 15 min to deactivate DNase. Then, 4 µl Maxima™ H Minus cDNA SynthesisMaster Mix was added to sample and gently mixed. cDNA synthesis was performed by GeneAmp 2700 thermocycler and program was set as:

25 °C 10 min → 50 °C 30 min → 85 °C 5 min

After cooling down to 4 °C, cDNA was filled up to 100 µL with RNase-free H_2O.

2.2.6.3 Quantitative Polymerase Chain Reaction (qPCR)

The mastermix for qPCR was prepared as follows:

Table 2.19 Preparation of mastermix for qPCR

RNase-free H_2O	2 µl
PrimerMix (as indicated in **2.1.2**)	1 µl
PowerUP SYBR® Green PCR Master Mix	5 µl
Total	8 µl

For each sample, 2 µl cDNA or non-template control and 8 µl of mastermix were pipetted into each well of a 96-well PCR plate. Measurement was performed by StepOne Plus Real-Time PCR Systems. Program was set as:

Table 2.20 Program of qPCR

Before Cycle		
UDG activation	50°C 2 minutes	Hold
Dual-Lock™ DNA polymerase	95°C 2 minutes	
Cycle		
Denature	95°C 15 seconds	40 cycles
Anneal/extend	62°C (IL-1β) or 64°C (18S rRNA) 1 minute	
Melting curve		
	95°C 15 seconds 60°C 1 minute + 0.3 °C / second 95°C 15 seconds	Hold

Data was analyzed with ΔΔCT (cycle threshold) method, and normalized to endogenous reference gene 18S rRNA.

2.3 Statistical Analysis

Statistical analysis was performed using SPSS Statistic 26 (IBM) and Graphpad Prism 9.0.1 (Prism). Data that was normal distributed was shown as mean ± standard deviation (SD), and tested by one-way analysis of variance (ANOVA) with Dunnett's multiple comparison post hoc test. Differences with $P < 0.05$ were considered statistically significant. Every experiment was performed at least three times or as indicated.

3. Results

3.1 Differentiation of THP-1 monocytes into macrophage-like cells

THP-1 cells, one of the most used monocytic cell line for inflammasome and pyroptopsis research, were treated with Phorbol-12-myristat-13-acetat (PMA), a Protein Kinase C activator, to induce differentiation from monocytes to macrophage-like cells (Daigneault, Preston, Marriott, Whyte, & Dockrell, 2010).

To determine the best condition for macrophage differentiation, THP-1 cells were treated as indicated in Table 2.16 for optimization. Adherent cells and suspension cells were collected and counted. Numbers of adherent cells increased by PMA in a time- and dose-dependent manner in 0 - 48 hours and 0 - 100 ng/ml, while numbers of cells in suspension decreased (Fig. 3.1 A and B). However cells treated with PMA for more than 48 hours or with concentrations higher than 100 ng/ml led to no more increase of adhesion.

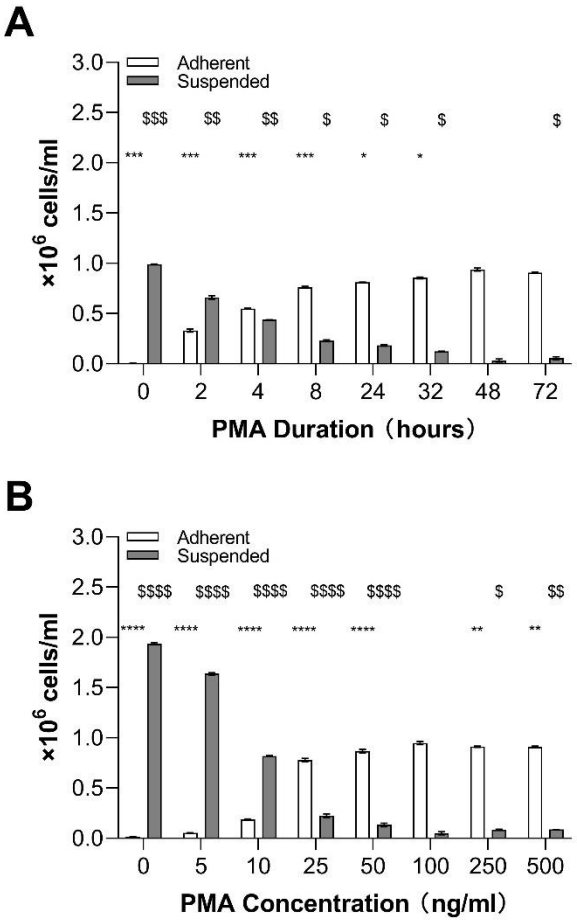

Figure 3.1 Optimization of PMA treatment for macrophage differentiation.

Adherent or suspension cell counts of PMA–treated THP-1 cells for 0-72 hours with 100 ng/ml PMA (A) and with 0 - 500 ng/ml for 48 hours (B). Supernant of PMA-treated cells were collected to obtain suspended cells, and adherent cells were collected by accutase detachment. N=3, *P < 0.05, **P < 0.01, ***P < 0.005, ****P < 0.001 comparing to suspended cell with PMA 48 hours (A) or 100 ng/ml (B), $ P < 0.05, $$ P < 0.01, $$$ P < 0.005, $$$$ P < 0. comparing to suspended cell with PMA 48 hours (A) or 100 ng/ml (B), respectively.

Before PMA treatment, THP-1 cells were suspended and round and after treatment, cells became adherent and multi-shaped, indicating a successful differentiation into macrophage-like cells. Microscopic assessment verified cell count results. The morphology of cells which were treated with 100 ng/ml PMA for 48 hours showed clear attachment in contrast to THP-1 monocytes, which were incubated with different PMA concentrations or other periods of time (Fig. 3.2).

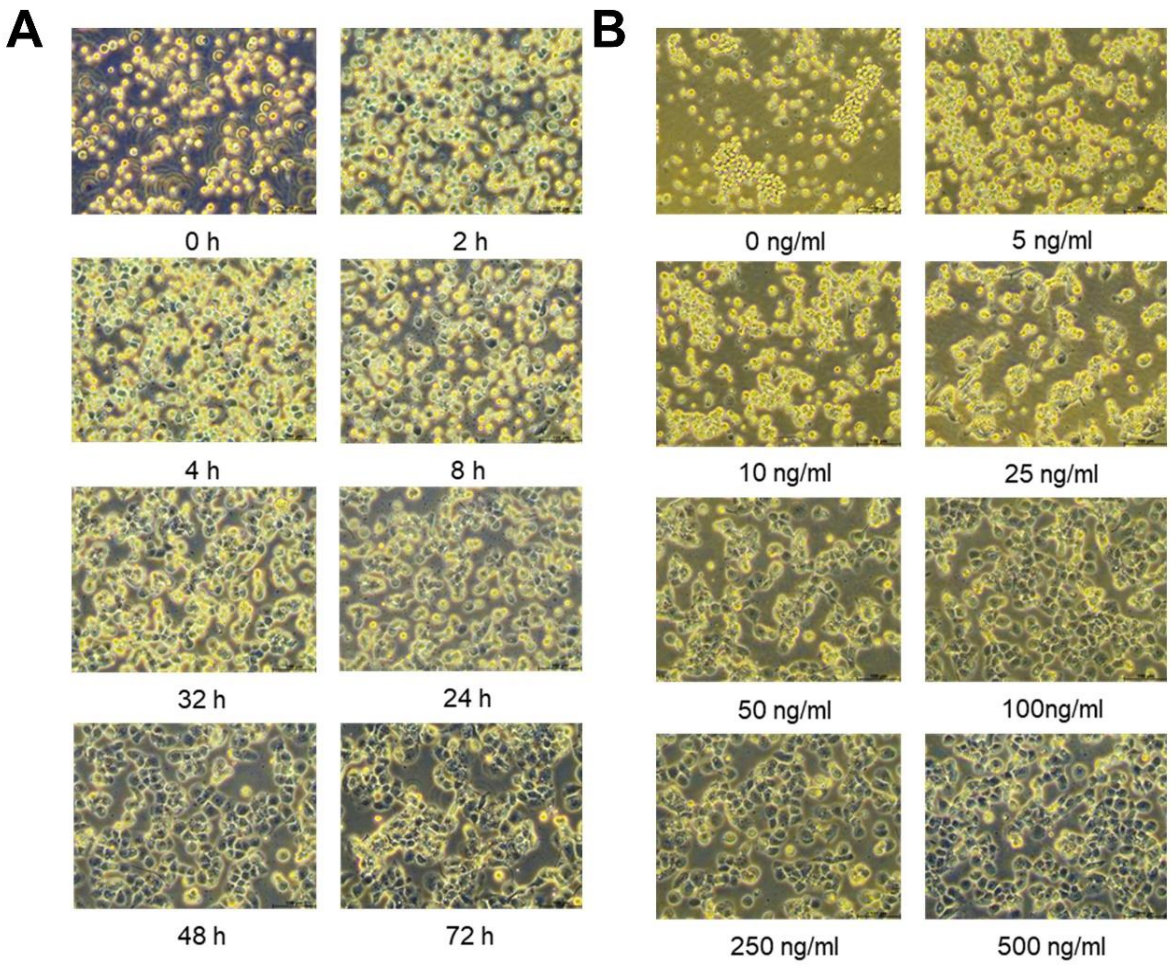

Figure 3.2 Morphology of PMA–treated THP-1 cells.
Microscope view of THP-1 cell morphology after 0 - 72 hours treatment with 100 ng/ml PMA (A) and 48 hours treatment with 0 - 500 ng/ml PMA (B).

To further prove the differentiation of THP-1 monocytic cells into a macrophage-like cell line, cells were stained for the macrophage maturation marker CD11b, which is expressed highly on macrophages, but only low on monocytes. Again,

the incubation with 100 ng/ml PMA for 48 hours induced an adequate expression of CD11b on the cell surface. Concentration higher than 100 ng/ml PMA did not further increase CD11b expression (Fig. 3.3).

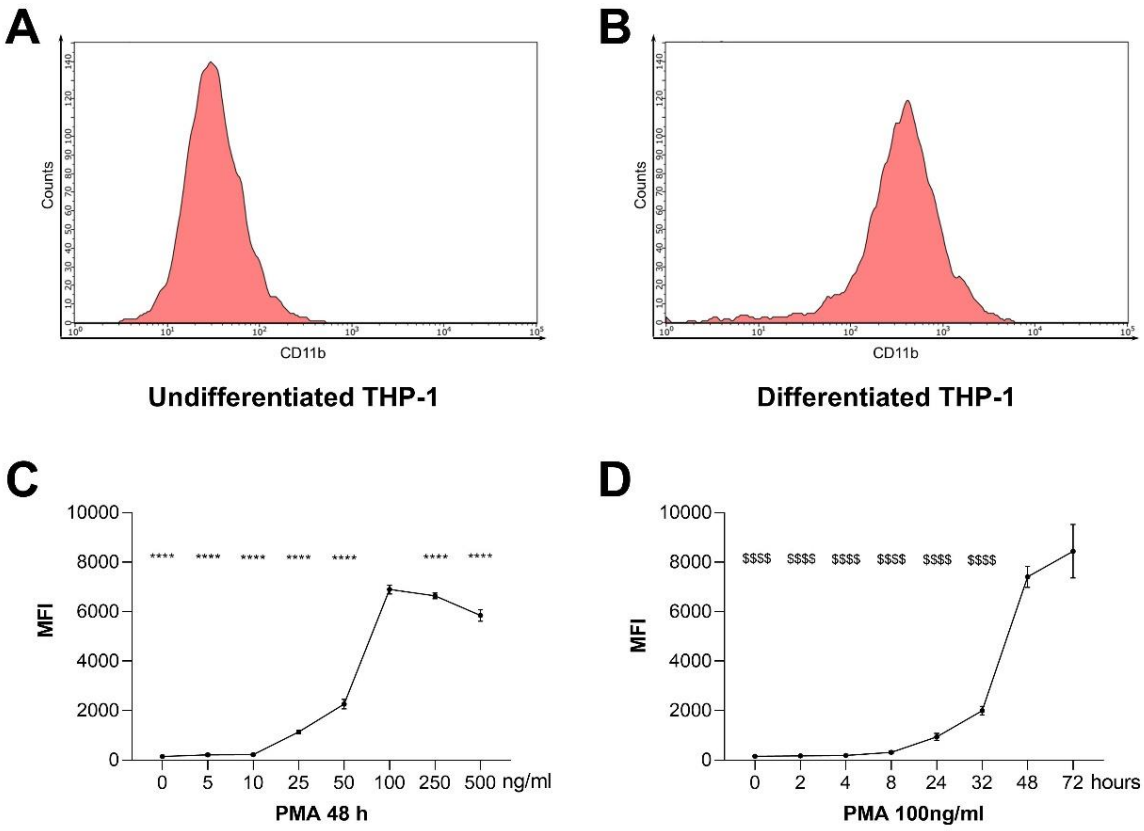

Figure 3.3 Cell surface CD11b expression on THP-1 cells after PMA treatment. CD11b expression on the cell surface of untreated THP-1 cells (A) and PMA–treated THP-1 cells after 48 hours incubation with 100 ng/ml PMA (B) and within treatment concentration (C) and duration (D) optimization. N=3, *P < 0.05, **P < 0.01, ***P < 0.005, ****P < 0.001 comparing to 100 ng/ml PMA for 48 hours, $ P < 0.05, $$ P < 0.01, $$$ P < 0.005, $$$$ P < 0.001 comparing to 48 hours of 100 ng/ml PMA treatment.

Altogether, these results confirm a 48 hours treatment with 100 ng/ml PMA to be the most efficient treatment conditions to induce differentiation from THP-1 monocytic cells into macrophage like cells. With this treatment pattern, cells were prepared for all subsequent experiments within these investigations.

3.2 Pyroptosis induction in THP-1 macrophage-like cells

Treatment with LPS and ATP is the most commonly used protocol for inducing pyroptosis in macrophages under experimental conditions. LPS is capable to prime the pyroptosis response of cells, ATP represents the 'second signal' to trigger inflammasome assembly and to activate caspase-1. In order to optimize conditions for pyroptosis induction in this experimental setting, LPS and ATP concentrations and treatment durations were titrated as shown in Table 2.17 and Table 2.18 and LDH assay was used as read-out.

Priming with 5 ng/ml LPS for 1 hour and subsequent 2.5 hours 5 mM ATP treatment was elaborated to induce LDH release of approx. 45 % compared to the high control (whole lysis of untreated THP-1 macrophage-like cells by 1 % Triton X-100) (Fig. 3.4 A, B). Higher LPS (Fig. 3.4 A) or ATP (Fig. 3.4 B) concentrations rather resulted in unspecific lysis, as determined in preparatory experiments (not shown). To define the most suitable treatment sequence to induce pyroptosis without strong time-dependent unspecific cytotoxicity, different consecutive sequences of LPS and ATP were tested (Table 2.18). Treatment for 1 hour with LPS (5 ng/ml) priming followed by 2.5 hours additional ATP (5 mM) treatment was the shortest duration to induce significant additive cytotoxicity (Fig. 3.4 C). LPS priming for 3 hours induced strong cell lysis regardless of ATP co-treatment (Fig. 3.4 D). Microscopic assessment confirmed pyroptosis induction in THP-1 macrophage-like cells. After LPS/ATP treatment, cells were swollen and detached (Fig. 3.5).

As a consequence of pyroptosis, IL-1β is expressed and released in the extracellular space. To demonstrate IL-1β production and release with the different time patterns of treatment, cell pellets and cell culture supernatants were collected for intracellular IL-1β flow cytometry staining and IL-1β ELISA, respectively.

Cells were primed with 5 ng/ml LPS for 1 hour, and incubated with or without 5 mM ATP for additional 1 – 3 hours (see Table 2.18). Flow cytometric analysis showed that LPS alone induced a time-dependet increase of (Pro-)IL-1β expression. Maturation and release did not happen without additional ATP. After co-treatment with ATP for 2.5 hours, intracellular IL-1β was significantly reduced compared to single LPS treatment, indicating maturation and release of IL-1β by ATP (Fig. 3.6 A), which could be confirmed by ELISA. As shown in Fig. 3.6 B,

LPS for 1 hour and additional ATP for 2.5 hours resulted in a significant increase of extracellular IL-1β concentration compared to LPS only treatment. Altogether, data from intracellular and extracellular IL-1β have clearly shown that this pyroptosis-specific cytokine was expressed and released after 5 ng/ml LPS priming for 1 hour and additional 5 mM ATP treatment for 2.5 hours. Based on the obtained results, these conditions were considered as appropriate to induce pyroptosis and to be used for the following experiments testing the effects of HC on pyroptosis.

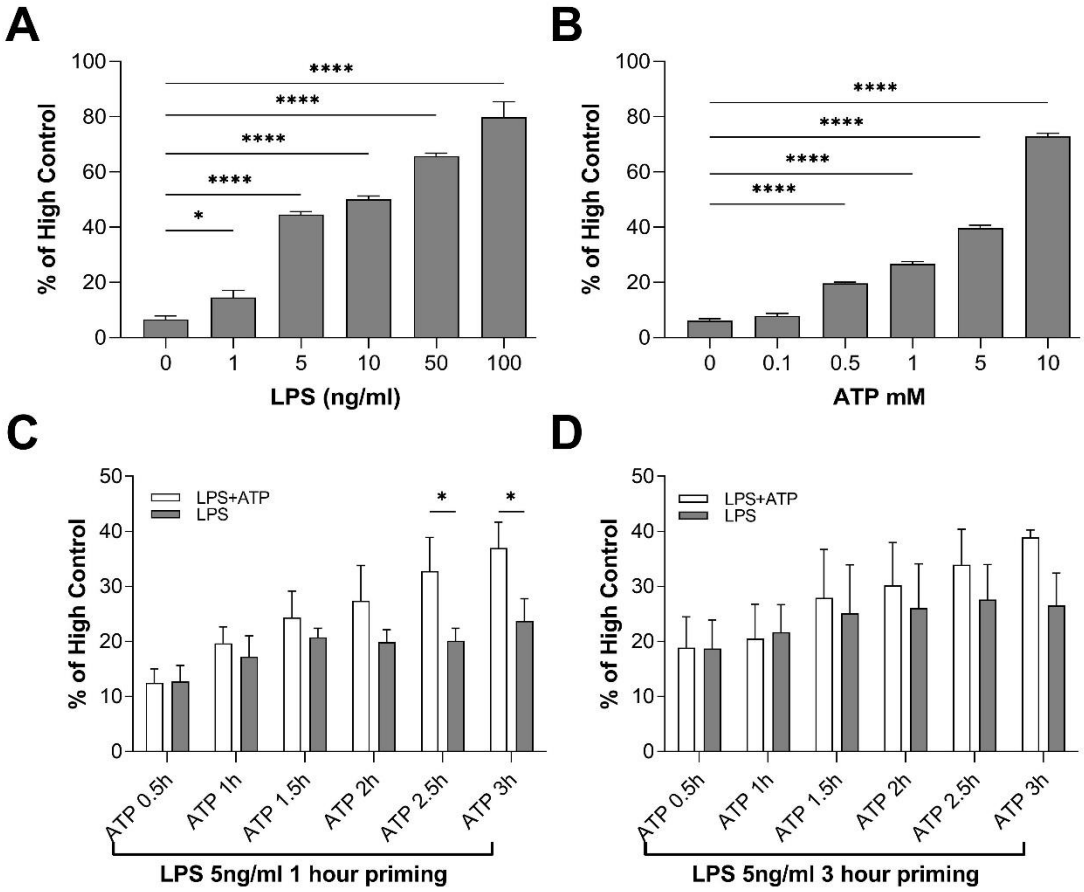

Figure 3.4 Extent of LDH release for optimization of pyroptosis induction by LPS and ATP.

LDH release after LPS/ATP co-treatment of THP-1 macrophage-like cells with different LPS priming concentrations but constant 5 mM ATP (A), different ATP co-treatment concentrations but constant 5 ng/ml LPS (B), LPS priming (5 ng/ml) for 1 hour with different durations of ATP (5 nM) co-treatment (C), LPS priming (5 ng/ml) for 3 hours with different ATP (5nM) co-treatment durations (D). LDH release showed extent of cell lysis (% of whole cell lysate/high control); N=3, *P < 0.05, **P < 0.01, ***P < 0.005, ****P < 0.001.

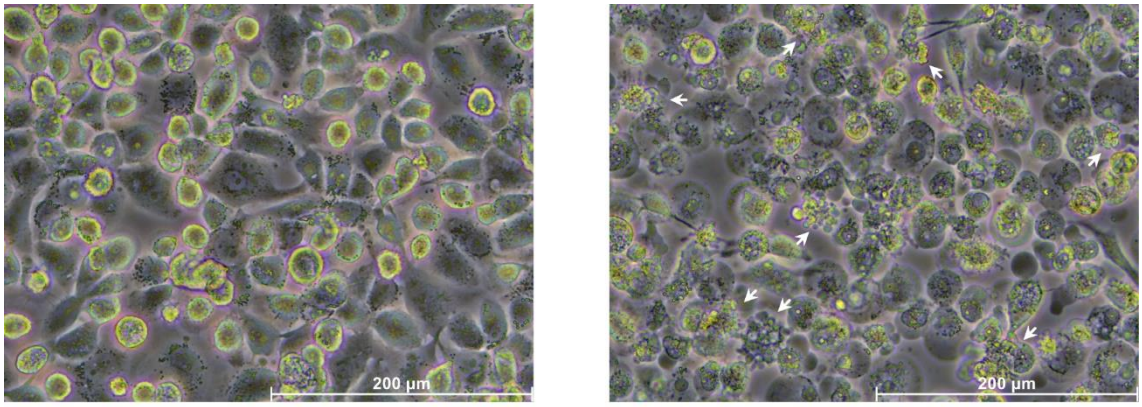

Figure 3.5 Morphology of THP-1 macrophage-like cells before and after pyrotosis induction.

Representative picture of microscopic assessment of morphology of untreated control cells and cells after pyroptosis induction with 1 hour LPS (5 ng/ml) and 2.5 hours ATP (5 nM), arrows show swollen or lysed cells, scale bar 200 µm.

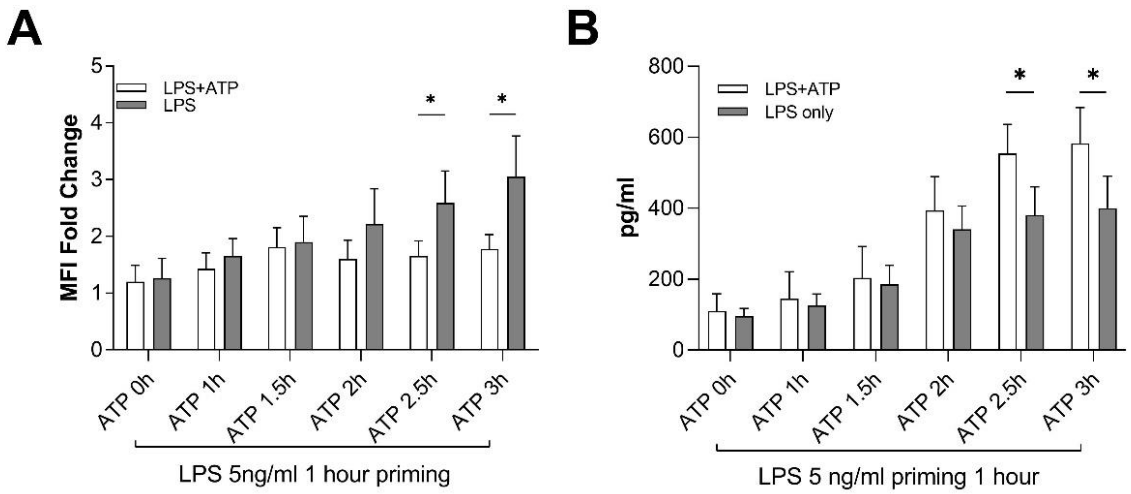

Figure 3.6 Intracellular and extracellular IL-1β concentration after optimized LPS and different ATP treatment conditions.

Expression of intracellular IL-1β (MFI) by flow cytometry (A) and of extracellular IL-1β concentration by ELISA (B) after pyroptosis induction with LPS (5 ng/ml) and ATP (5 mM) at different treatment time patterns. N=3; *P < 0.05.

3.3 Effects of hydrocortisone on pyroptosis induction and cell death

To investigate the effects of HC in different concentrations on pyroptosis, different treatment regimens were applied (Fig. 3.7). An „acute exposure“ approach reflected a sudden increase in HC concentration, as it is the case for drug administration at the onset of infection. The „chronic exposure“ mimicked a physiological state with continuously high HC concentrations such as in very stressed patients or under continuous HC therapy. A „physiological control“ was set to simulate a physiological HC concentration in human blood (Feuerecker et al., 2013), and a „blank control“ was additionally set as a normal cell culture condition.

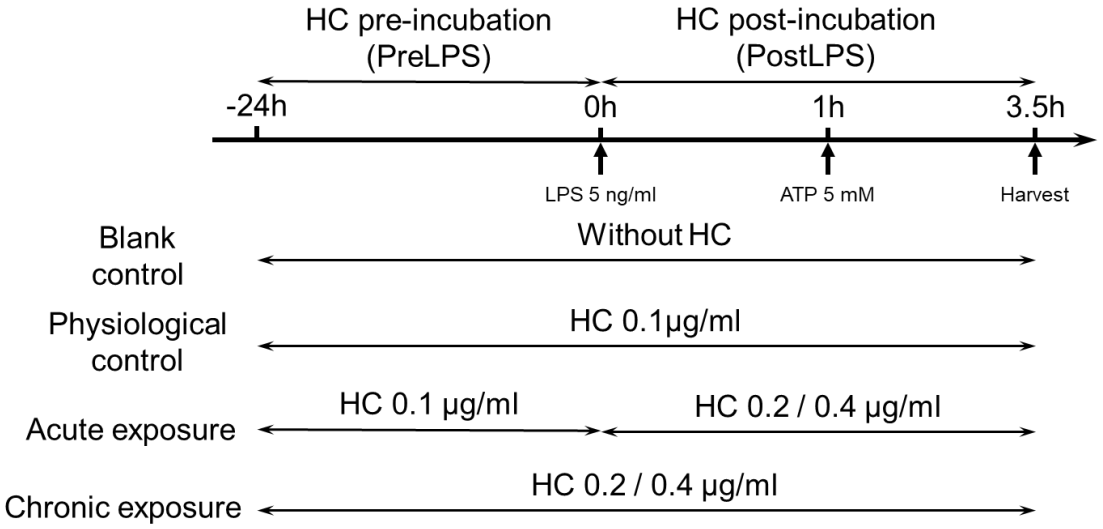

Figure 3.7 Time scheme of hydrocortisone treatment.

For analysis of cell lysis due to treatments, cell culture supernatants were collected for LDH release measurements.

Compared to blank control with no HC, the physiological control with 0.1 µg/ml HC displayed a reduction of LPS/ATP induced LDH release, which indicated a protective effect of HC regarding cell death, even at low concentrations. Under acute exposure, LDH release was not affected by increasing HC concentrations (Fig. 3.8 A). However, under chronic HC exposure, LDH release was further decreased (Fig. 3.8 B), indicating that high HC concentrations before pyroptosis

induction protect cells from lysis, wherease acute application of high HC, when pyroptosis is initiated has no protective effects.

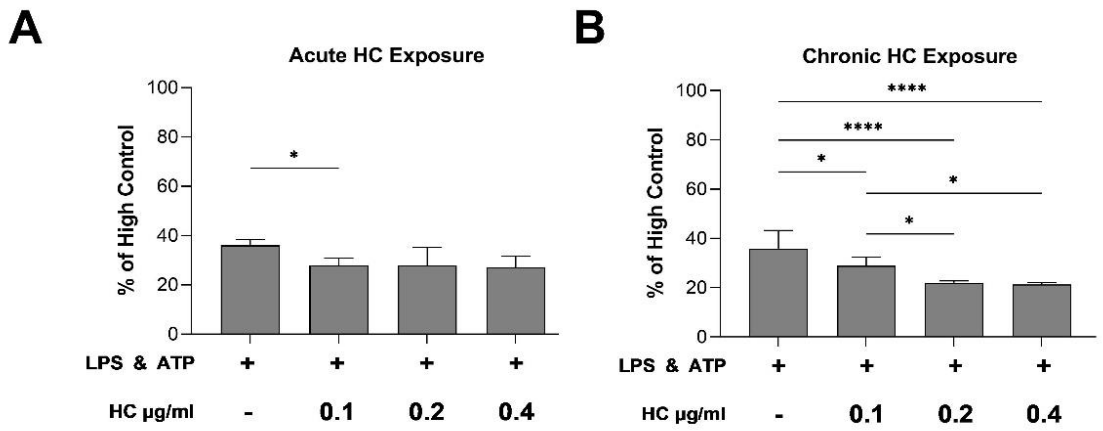

Figure 3.8 LPS/ATP induced LDH release under acute or chronic HC exposure.

Upon pyroptosis induction with LPS (5 ng/ml) and ATP (5 mM), THP-1 macrophage-like cells were either treated with increasing HC concentrations from 0.1 µg/ml to 0.2 µg/ml or 0.4 µg/ml (A, acute exposure) or treated constantly with HC (0.1, 0.2, 0.4 µg/ml) 24 hours prior to pyroptosis induction and afterwards (B, chronic exposure). N=5, *P < 0.05, **P < 0.001, ***P < 0.005, ****P < 0.001.

Since pyroptosis is defined as caspase-1 dependent cell death, caspase-1 and PI positive cells were measured by flow cytometry after HC treatment.

Pyroptosis was induced in approximately 30 % of the blank control cells and the percentage was significantly reduced in the physiological control. Acute exposure to high HC concentrations showed no reduction compared to blank control and even increased values compared to the physiological control (Fig. 3.9 A). Under chronic HC exposure, caspase-1/PI double-positive cells decreased significantly compared to blank control and physiological control in a dose-dependent manner (Fig. 3.9 B). This suggests that the application of high HC at the onset of pyroptosis abolishes the protective effect of 0.1 µg/ml HC regarding macrophage cell death, whereas chronically elevated HC concentrations further reduce cell death. Proportion of PI positive cells which indicated death cells show similar results as LDH release. Cell death was reduced in physiological control compared to blank control, but increased HC under acute exposure did not further protect cell from

death (Fig. 3.9 C); under chronic exposure, however, the protective effect was dose-dependently increased (Fig. 3.9 D).

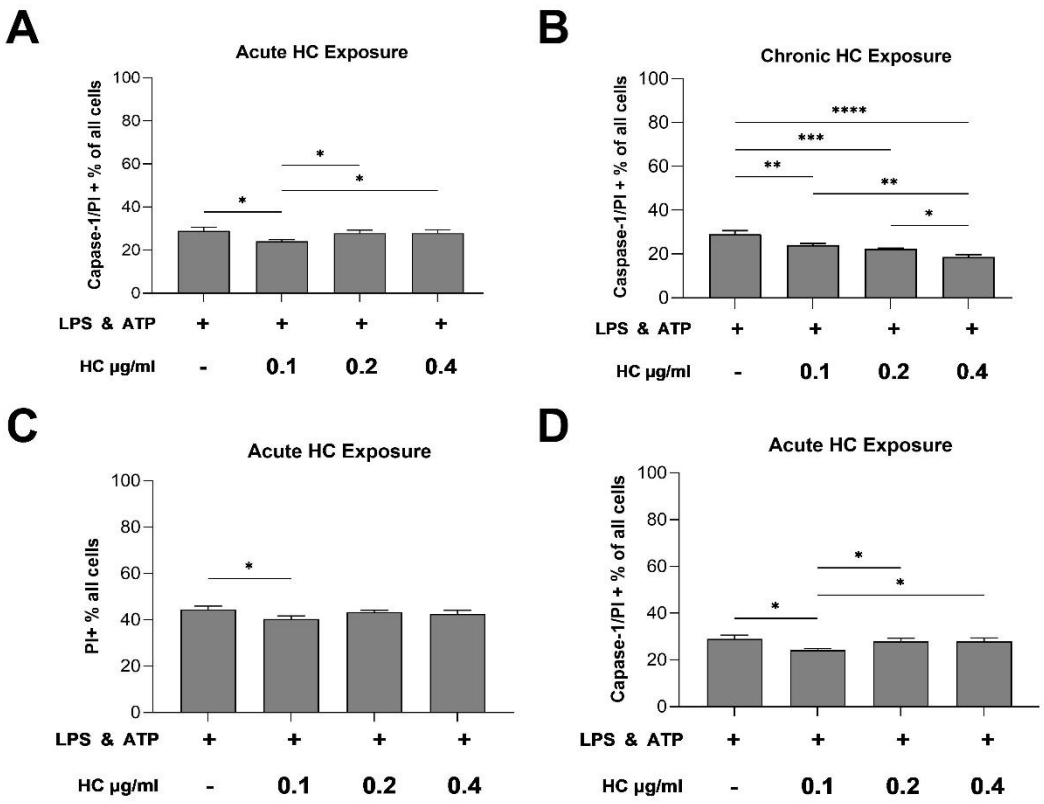

Figure 3.9 Pyroptosis detection by caspase-1/PI double staining.

Staining of active caspase-1/PI$^+$ THP-1 macrophage-like cells after pyroptosis induction with LPS (5 ng/ml) and ATP (5 mM) under acute HC exposure (A) or chronic HC exposure (B), and PI$^+$ under acute HC exposure (C) or chronic HC exposure (D) Displayed are mean values +STD of the percentage of double-positive caspase-1/PI or single PI-positive cells among measured cells. N=3, * P < 0.05, ** P < 0.001, *** P < 0.005, ****P< 0.001.

3.4 Underlying mechanism of pyroptosis protection by hydrocortisone and outcomes in different treatment patterns

3.4.1 Effect of different HC exposures on the NF-κB signaling pathway

The NF-κB signaling pathway plays an important role on immune response against pathogen infection. Its activation induces the expression of pro-inflammatory cytokines, such as of IL-1β (Zhang et al., 2016). To investigate the effects of acute and chronic HC exposure on NF-κB signaling pathway activation in pyroptosis, the phosphorylation of the NF-κB subunit p65 and its and nuclear translocation was assessed.

Phosphorylation of the p65 subunit was determined by western blot. As shown in Fig. 3.10, acute HC exposure had no alleviating effect on p65 phosphorylation. However, chronic exposure of HC dose dependently suppressed p65 phosphorylation, indicating reduced activation of NF-κB signaling pathway (Fig. 3.10).

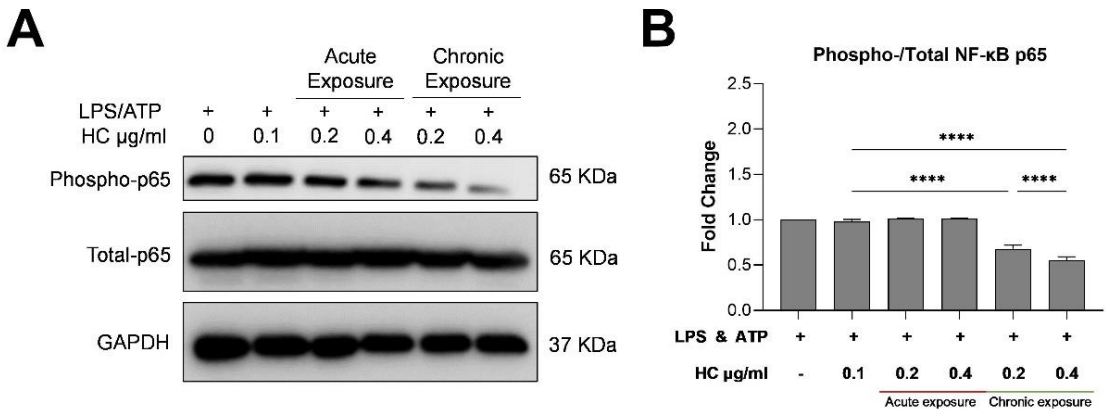

Figure 3.10 Effect of acute or chronic HC exposure on NF-κB p65 phosphorylation. Representative western blot of phosphorylated- and total-NF-κB p65 and of housekeeping GAPDH (A) and semiquantitative analysis of phospho/total p65 ratio (B). The ratio between phospho and total p65 represents the amount of cleaved protein. Pyroptosis was induced by LPS (5 ng/ml) and ATP (5 mM) under acute or chronic HC exposure. N=3, *P < 0.05, **P < 0.001, ***P < 0.005, ****P < 0.001.

In addition to NF-κB p65 phosphorylation, its nuclear translocation was analysed by immunocytochemical staining. Laser scanning microscopy showed that under acute HC exposure nuclear translocation of NF-κB p65 subunit was not affected (Fig. 3.11 A⑤⑦ & B) compared to both controls (Fig. 3.11 A③④ & B), which corresponds to the maintained p65 phosphorylation in western blot. Under chronic HC exposure, translocation of p65 was dose-dependently decreased (Fig. 3.11 A ⑥⑧ & B).

Both results of phosphorylation and translocation of NF-κB p65 indicate that high-dose HC inhibits NF-κB signaling activation only under chronic exposure and not under short-term acute exposure.

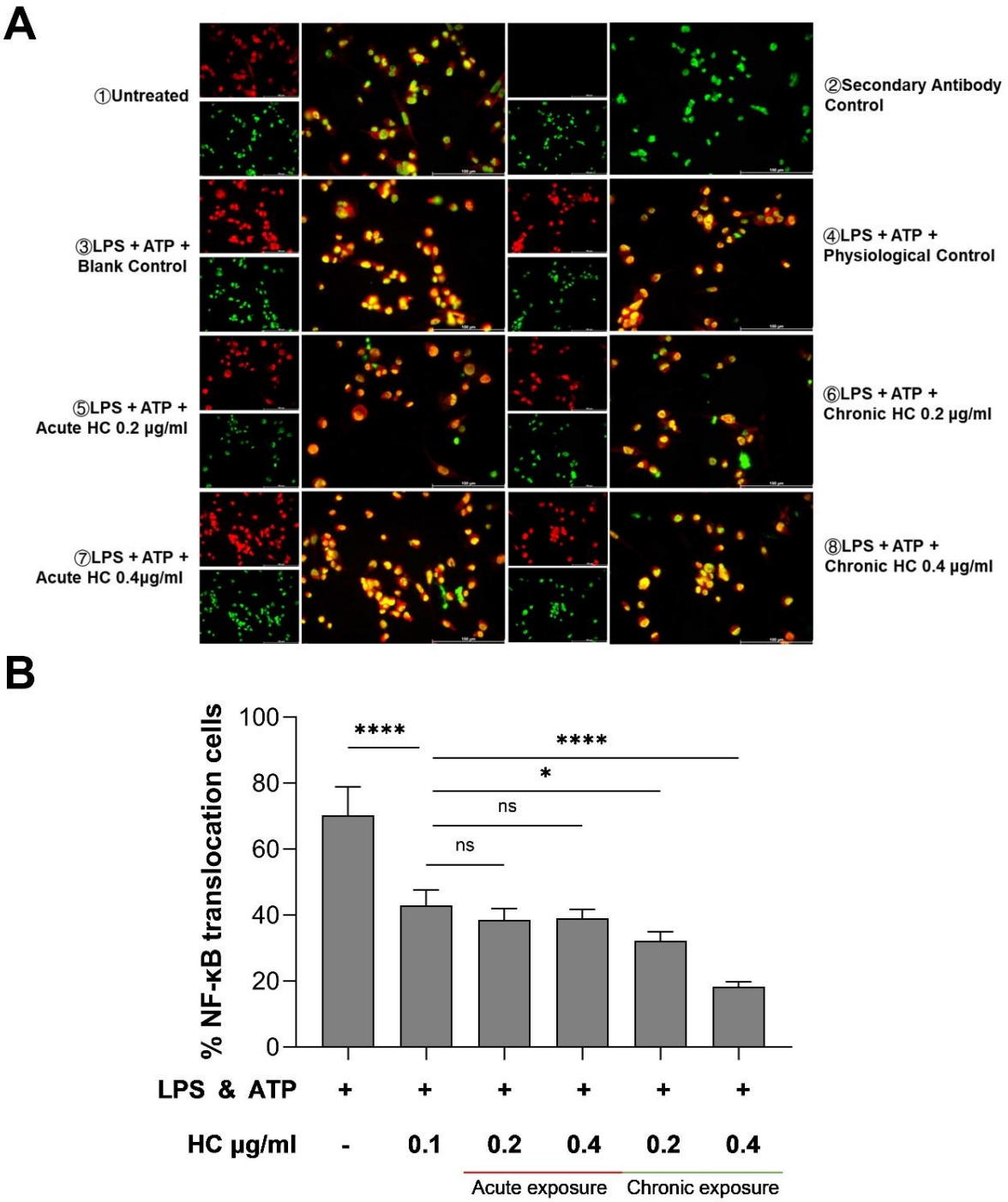

Figure 3.11 Effect of acute or chronic HC exposure on NF-κB p65 translocation. Representative immunocytochemical staining of NF-κB p65 nuclear translocation (A) and statistical analysis (B). Red: NF-κB p65, green: nuclear DNA staining; 100 cells from three different views were counted with NF-κB p65 and nuclear DNA overlay (yellow) considered as cells with translocation. N=3, *P < 0.05, **P < 0.01, ***P < 0.005, ****P < 0.001.

3.4.2 Modulation of pyroptosis-associated proteins by different hydrocortisone exposure patterns

3.4.2.1 The role of HC exposure patterns on the key cytokine IL-1β

The production of IL-1β relies on the priming phase (step 1) and maturation and release within the execution phase (step 3). To explore the effects of different HC-exposure patterns on IL-1β expression, mRNA levels were determined by qRT-PCR, intracellular pro-IL-1β and cleaved IL-1β was quantified by western blot and flow cytometry and release of mature IL-1β was measured by ELISA in cell culture supernatants.

qRT-PCR revealed that IL-1β mRNA transcription was independent of HC treatment, irrespective of the dosage (Fig 3.12), similar observations were made by intracellular pro-IL-1β staining (Fig. 3.13).

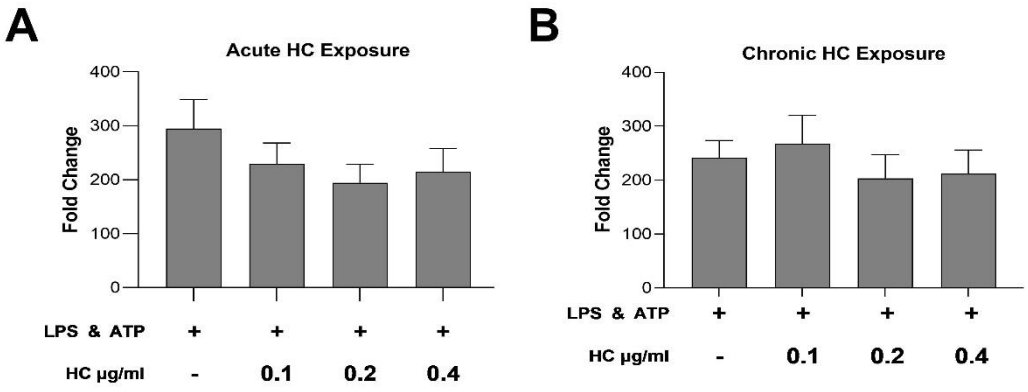

Figure 3.12 IL-1β mRNA levels after acute and chronic HC exposure.
mRNA levels of IL-1β under acute (A) or chronic (B) HC exposure. Bars represent fold change to untreated controls, N=3.

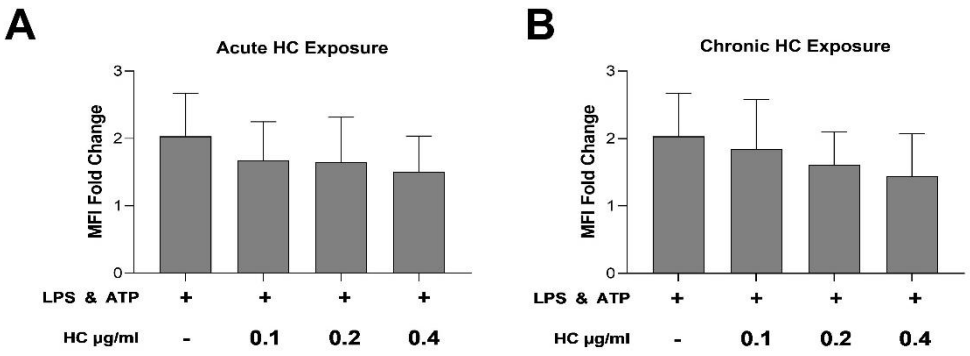

Figure 3.13 Abundance of intracellular IL-1β after acute and chronic HC exposure.
Flow cytometric measurement of intracelluar IL-1β under acute (A) or chronic (B) HC exposure. Bars represent fold change in MFI to untreated control, N=3.

To further clarify the HC effect on pro-IL-1β and mature IL-1β, western blots were performed and extent of protein cleavage was assessed by cleaved/Pro-IL-1β ratio. Under acute HC exposure the ratio was strongly decreased (Fig. 3.14 B) with weak mature IL-1β signal (Fig. 3.14 A), suggesting that the majority of mature IL-1β was released. Together with maintained cell lysis (Fig. 3.8), this further indicates that acute HC exerts no protective effect regarding IL-1β release and pyroptosis.

After chronic HC exposure, the ratio between cleaved and pro-form IL-1β was also dose-dependently decreased but still with a strong signal of mature IL-1β (Fig. 3.14). This observation fostered the assumption, that under chronic HC exposure, cells are protected from lysis (Fig. 3.8) and so, IL-1β remains in the cells.

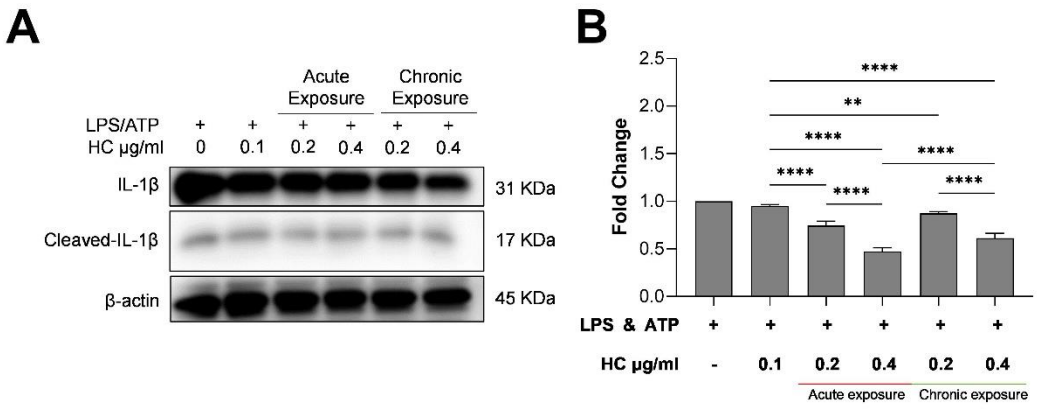

Figure 3.14 IL-1β cleavage after acute and chronic HC exposure.
Representative western blot (A) of IL-1β, cleaved (mature) IL-1β and β-actin as a housekeeping protein under acute or chronic HC exposure and semiquantitative analysis (B). Ratio between cleaved and Pro-IL-1β represent amount of cleaved protein. N=3 *P < 0.05, **P < 0.001, ***P < 0.005, ****P < 0.001.

Release of mature IL-1β is the most important step of pyroptosis, as this cytokine activates nearby immune cells. ELISA measurements revealed that under acute HC exposure IL-1β concentrations dose-dependently increased, reaching almost blank control values at 0.4 µg/ml (Fig. 3.15 A). Upon chronic HC exposure IL-1β concentrations decreased in a dose-dependent manner (Fig. 3.15 B), indicating suppression of IL-1β release by anti-inflammatory effects of HC on macrophages.

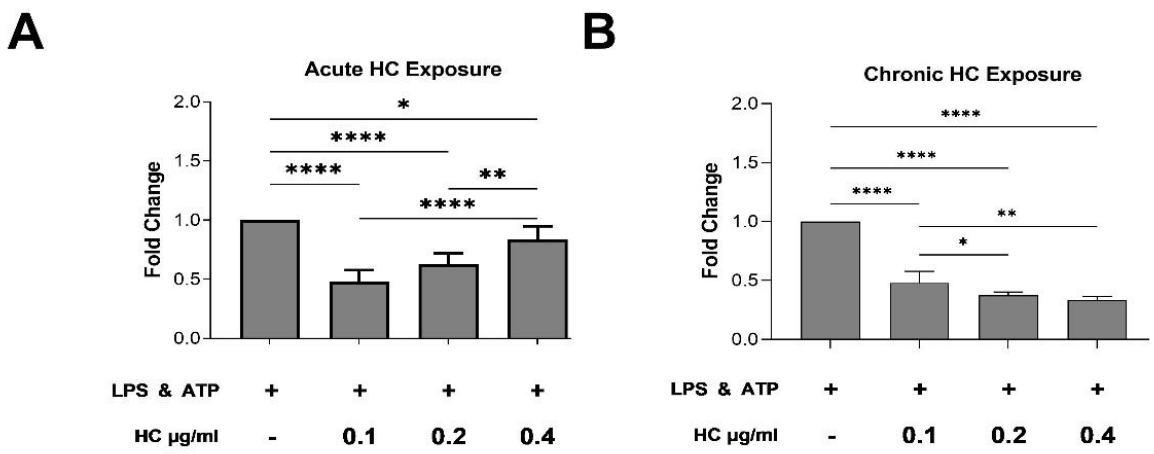

Figure 3.15 Effect of acute and chronic HC exposure on IL-1β release.
IL-1β ELISA of cell culture supernatant under acute (A) or chronic (B) HC exposure. Bar charts show fold change of IL-1β concentrations (pg/ml) compared to blank control (LPS & ATP +). N=3 * P < 0.05, ** P < 0.001, *** P < 0.005, ****P < 0.001.

In summary, HC chronic exposure dose-dependently protected macrophages from pyroptosis and limited IL-1β maturation and release. Acute exposure didn´t result in lysis protection and promoted IL-1β release instead.

3.4.2.2 Impact of HC on inflammasome forming proteins

The inflammasome is the central component to activate pyroptotic cell death. In LPS/ATP induced pyroptosis, NLRP3, ASC and caspase-1 assemble to the NLRP3 inflammasome. Gasdermin D is, same as IL-1β, a protein which is cleaved by the NLRP3 inflammasome. Upon proteolytic activation, it aggregates with other cleaved gasdermin D proteins, which leads to pore formation on the cell membrane and ultimately to cell lysis. Western blot analysis of NLRP3, gasdermin D (Gasdermin D-NT) and caspase-1 showed, that under acute HC exposure, NLRP3, gasdermin D-NT and cleaved-caspase-1 protein expression was not affected (Fig. 3.16 A-D). With chronic HC however, expression of NLRP3 as well as of gasdermin D-NT and cleaved-caspase-1 were dose dependently decreased (Fig. 3.16 A-D).

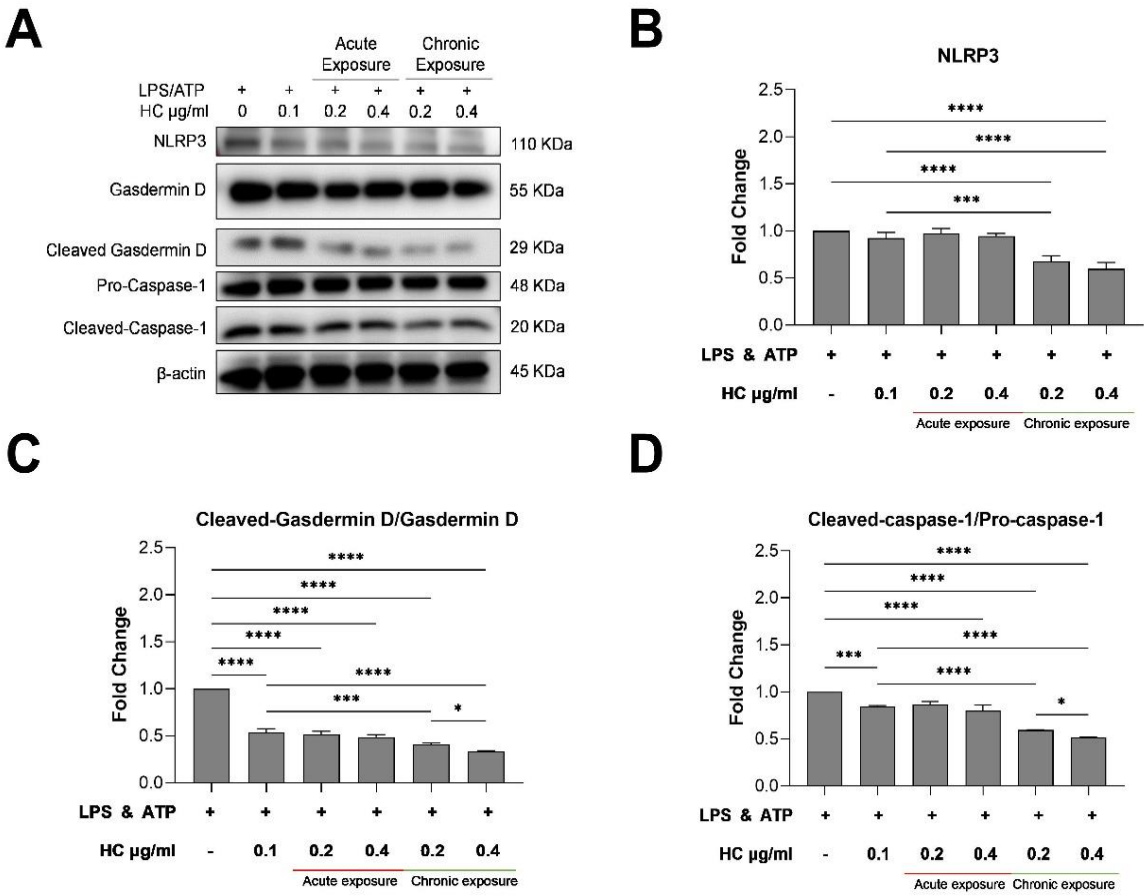

Figure 3.16 Western blot on impact of acute or chronic HC on inflammasome forming proteins and gasdermin D cleavage.

Representataive western blot of inflammasome forming proteins (A) and semiquantitative fold expression change of NLRP3 expression (B), cleaved-/Pro-gasdermin D ratio (C) and cleaved-/Pro-caspase-1 ratio (D). N=3, *P < 0.05, **P < 0.001, ***P < 0.005, ****P < 0.001.

Similar to extracellular IL-1β levels, caspase-1 concentration in cell culture supernatants was dose-dependently decreased under chronic HC exposure (Fig. 3.17 B). In the acute exposure approach, the inhibitory effect of the physiological control was abolished (Fig. 3.17 A).

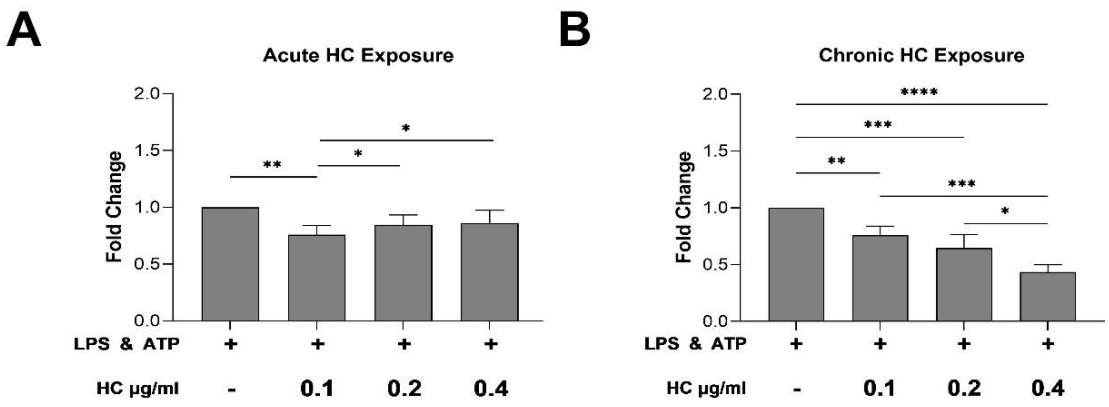

Figure 3.17 Effect of acute or chronic HC exposure on extracellular caspase-1 concentration.

Caspase-1 concentration in cell culture supernatants measured by ELISA under acute (A) or chronic (B) HC exposure. Bar graphs represent fold change to blank control. N=5, * P < 0.05, ** P < 0.001, *** P < 0.005, ****P < 0.001.

3.4.2.3 Impact of HC on inflammasome assembly

With the presence of an execution signal such as ATP, inflammasome starts to assemble and then activates caspase-1 for cleavage of pyroptosis-related proteins. To investigate inflammasome assembly under different HC treatment regimens, Co-immunoprecipitation (Co-IP) of NLRP3 and ASC was performed. Under acute HC exposure, the ASC signal was unchanged high as in the physiological control (Fig 3.18 A IP lane 2, 3, 4 and B). However, within chronic HC exposure, less ASC was co-precipitated with NLRP3 (Fig 3.18 A IP lane 2, 5, 6 and B). Immunocytochemistry staining showed similarly, that in comparison to the phsiological control, acute HC exposure did not change the extent of inflammasome formation (Figure 3.18 C ②③⑤), however, chronic HC exposure decreased inflammasome formation (Figure 3.18 C ②④⑥).

Altogether, results derived from these investigations indicate that a chronic high-dose HC exposure inhibited pyroptosis, whereas an acute HC exposure promoted pyroptosis via maintaining and fostering inflammasome assembly.

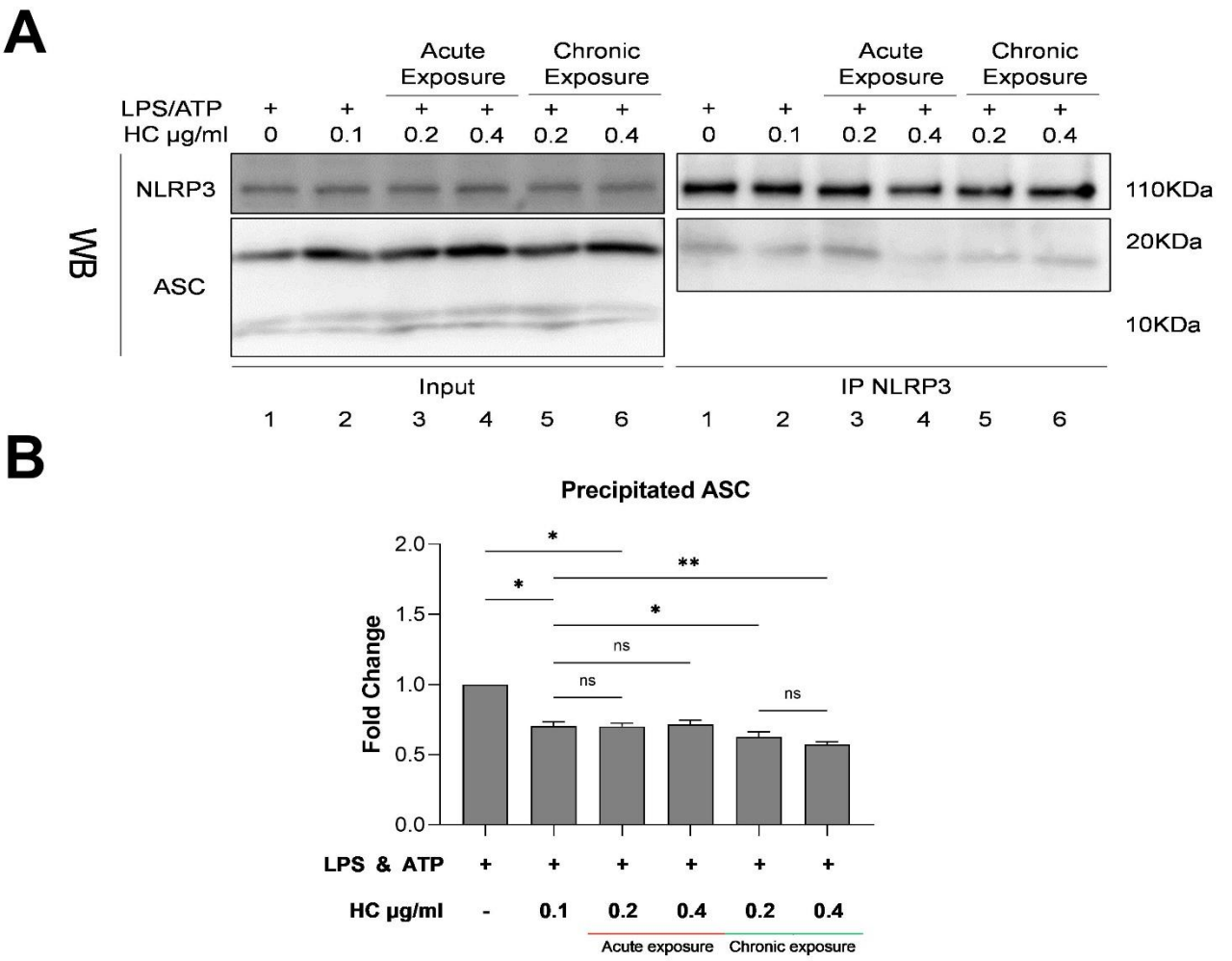
A
Acute Exposure
Chronic Exposure
Acute Exposure
Chronic Exposure
LPS/ATP + + + + + + + + + + + +
HC μg/ml 0 0.1 0.2 0.4 0.2 0.4 0 0.1 0.2 0.4 0.2 0.4
NLRP3
ASC
WB
110KDa
20KDa
10KDa
Input
IP NLRP3
1 2 3 4 5 6 1 2 3 4 5 6
B
Precipitated ASC
Fold Change
2.0
1.5
1.0
0.5
0.0
*
**
*
*
ns
ns
ns
LPS & ATP + + + + + +
HC μg/ml - 0.1 0.2 0.4 0.2 0.4
Acute exposure
Chronic exposure
C
①LPS + ATP + Blank Control
②LPS + ATP + Physiololgical Control
③LPS + ATP + Acute HC 0.2
④LPS + ATP + Acute HC0.4
⑤LPS + ATP + Chronic HC 0.2
⑥LPS + ATP + Chronic HC0.4
10 μm

Figure 3.18 Effect of HC acute or chronic exposure on inflammasome assembly after LPS/ATP induced pyroptosis.

Representative co-immunoprecipitation blot (A) of NLRP3 and ASC and semiquantitative analysis of precipitated-ASC signal expressed as fold change to values of physilogical control (B). Representative immunocytochemistry staining (C) of NLRP3 (red) and ASC (green), arrow shows colocalization of NLRP3 and ASC, which are regarded as inflammasome (yellow). N=3, * $P < 0.05$, ** $P < 0.001$, ****$P < 0.001$, scale bar 10 µm.

4. Discussion

Cortisol is one of the most important stress hormones and its synthetically produced analog, which is used as a drug against inflammation, it´s termed hydrocortisone (HC). Recent studies demonstrated that HC has both anti- and pro-inflammatory effects (Dhabhar, 2002; Kadmiel & Cidlowski, 2013). In the present *in vitro* study, the impact of HC in different concentrations and treatment regimens was tested on LPS/ATP induced pyroptosis of THP-1 macrophage-like cells. By this, insights into the therapeutical potential of HC on macrophages were gathered in dependence of either acute administration or chronically high levels.

It was observed that an acute or chronic HC exposure affects pyroptosis very differently: acute HC exposure, where increase in HC concentration occured concomitantly with pyroptosis induction, did not inhibit pyroptosis and even abolished alleviating effects of 0.1 µg/ml HC pre-exposure. Moreover, inflammasome assembly and release of IL-1β in the extracellular space was promoted compared to the physiological control, while macrophages didn´t show enhanced cell membrane rupture and cell lysis, which may suggest a hyperactive state of THP-1 macrophage-like cells (Evavold et al., 2018). Chronic HC exposure however, in which HC levels were already high 24 hours before pyroptosis induction inhibited pyroptosis in THP macrophage-like cells, protected from cell lysis, but also reduced promotion of inflammation. Expression and release of IL-1β were clearly inhibited.

4.1 THP-1 macrophage-like cells represent an ideal model for LPS/ATP induced pyroptosis

THP-1 is the first established human monocytic cell line derived from acute monocytic leukemia (Tsuchiya et al., 1980), and it is a widely used model for *in vitro* monocyte and macrophage research. THP-1 cells are round suspension cells that can be induced into adherent, multishaped macrophage-like cells by various stimuli such as PMA or 1,25-dihydroxyvitamin D3 (Fleit & Kobasiuk, 1991; Tsuchiya et al., 1982). PMA-induced THP-1 macrophage-like cells share most similarity with primary monocyte derived macrophages (Daigneault et al., 2010), however, dose and treatment duration for differentiation differ strongly among

studies with concentration ranges of 40-200 ng/ml and treatment durations of several hours up to 3 days (Daigneault et al., 2010; Fleit & Kobasiuk, 1991; Kohro et al., 2004).

In optimization experiments, an incubation of THP-1 cells with 100 ng/ml PMA for 48 hours was identified to induce an appropriate differentiation into macrophage-like cells. Under this condition, the proportion of adherent cells was highest with a typical multishaped morphology of macrophages (Daigneault et al., 2010), and cell surface marker CD11b expression (Maeß, Wittig, Cignarella, & Lorkowski, 2014).

THP-1 macrophage-like cells represent a cell culture model for pyroptosis research (Shrivastava, Valenzuela Leon, & Calvo, 2020). In this setting, pyroptosis was induced by LPS and ATP, with LPS representing the priming stimulus and ATP, which is physiologically acting as a DAMP as the second stimulus. In literature, treatment dosages and conditions differ strongly. In one study for instance, bone marrow-derived macrophages from mice were treated with 1 µg/ml LPS for 3 hours followed by 5 mM ATP for 1 hour to induce pyroptosis and high IL-1β release (Di et al., 2018). Another study reported that pyroptosis was efficiently induced by 100 ng/ml LPS (Sordi, Panahipour, Kargarpour, & Gruber, 2022). Because of these various settings, optimized treatment conditions for pyroptosis induction were also elaborated in the present study. Priming with 5 ng/ml LPS for 1 hour followed by additional incubation with 5 mM ATP turned out to induce about 45 % cell lysis and upregulate high IL-1β production and release.

With these optimizmed treatment conditions, the impact of an acute or chronic HC exposure on inflammasome activation and pyroptosis was investigated.

4.2 Hydrocortisone influenced response of THP-1 macrophage-like cells

The presence of HC in *in vitro* experiments creates conditions closer to *in vivo* conditions, as without HC. For instance it has been reported in an allergy model, that during dendritic cell induced T cell activation, presence of HC downregulates Th1 but not Th2 responses (Bellinghausen et al., 2001), leading to pro-allergic

response. Lacking HC during stimulation would reduce allergic effects due to unsuppressed Th1 response. A study on THP-1 macrophage-like cells showed that cell cultivation with HC induces CD163 expression regardless of LPS stimulation which an associated M2-like phenotype (Mendoza-Cabrera et al., 2020), whereas polarization to M1-like macrophages occurs in the absence of HC.The effect of M2 polarization in this case would be ignored resulting in uncomparable between animal/human observation and cell culture model. Hence, understanding HC in cell culture - especially immune cell culture- helps to reveal comparable responses of macrophages/macrophage-like cells *in vivo* and *ex vivo*.

Results from the present investigation showed that THP-1 macrophage-like cells from blank control were more sensitve to LPS/ATP treatment compared to cells under physiological control HC concentrations (0.1 µg/ml). Higher cell death (general or pyroptotic), more IL-1β release, more caspase-1 activation and more NF-κB translocation after pyroptosis induction in was observed blank control cells. Without HC, the immune response of THP-1 macrophage-like cells might be overestimated and inaccurate.

This finding illustrated that HC influenced macrophage immune response *in vitro* as expected. Results from the present study and other pulished studies altogether suggested that HC is crucial in immune cell responses. Results from cultivation systems lacking HC might lead to an increase and shift of responses of activated immune cells, which would cause incomparable between *in vitro* and *in vivo* experiments.

4.3 Different hydrocortisone exposure patterns influence NF-κB signaling pathway and (pro-)IL-1β expression.

The pro-inflammatory cytokine IL-1β represents one key downstream inflammatory product in pyroptosis and the NF-κB signaling pathway is crucial to regulate (pro-)IL-1β expression. Upon stimulation, LPS binds to cell membrane TLRs like TLR2 or TLR4 on macrophages (Needham & Trent, 2013), which leads to NF-κB phosphorylation and translocation into the nucleus to regulate gene transcription (Bauernfeind et al., 2009). However, not only expression of (pro-)IL-1β is upregulated, but also of gasdermin D (Bauernfeind et al., 2009; X. Liu et al., 2016) which is indispensable for protein maturation and pore formation.

HC is an anti-inflammatory drug, which exerts its function via GR activation (Whitfield, Jurutka, Haussler, & Haussler, 1999). Activated GRs translocate into the nucleus and negatively interact with the NF-κB p65 subunit to inhibit transcription of pro-inflammatory genes (Liden, Delaunay, Rafter, Gustafsson, & Okret, 1997; Reily, Pantoja, Hu, Chinenov, & Rogatsky, 2006), thereby slowing down transcription by genomic effects. Rapid non-genomic effects work through interaction with other signaling pathways, for example p38 MAPK signaling pathway, which was shown to directly interact with GR (Busillo & Cidlowski, 2013).

The presented results indicate that chronic HC exposure dose-dependently suppressed NF-κB p65 subunit phosphorylation and nuclear translocation. Interestingly, the expression of pro-IL-1β was not significantly reduced by HC, suggesting an involvement of other signaling pathways for pro-IL-1β expression such as AP-1 (Wan et al., 2022).

Acute high-dose HC exposure didn´t result in reduced NF-κB p65 subunit phosphorylation and translocation compared to physiological control, which was mirrored by constant pro-IL-1β levels. Moreover, mature IL-1β and its release was even increased which suggests on the one hand pro-inflammtory actions by acute HC exposure and on the other hand that the effects which are caused by pyroptosis induction (LPS and ATP) occur faster than the transcriptional inhibition of pro-inflammatory genes by HC.

Pro-inflammatory functions of GCs were observed also by other researchers. Liu et al. showed that a 24 hours pretreatment of BV2 microglial-like cells with 50 nM corticosterone resulted in an enhanced translocation of NF-κB to the nucleus in response to LPS priming (J. Liu, Mustafa, Barratt, & Hutchinson, 2018). In addition to that, acute stress, which is associated with high cortisol levels (Davis, Engeland, & Murdock, 2020) is likewise capable to induce proinflammatory cytokines and signaling pathways (Dhabhar, 2002). The mechanisms of action of immune-enhancing effects of HC were not fully elucidated by now. However, one sociological experiment has found that under stress conditions, blood IL-1β level doubles right after onset of stress (Tait, Aisbett, Hall, & Main, 2019). Observations in boxers after boxing matches showed similar results, with having more than two-fold increase in cortisol and IL-1β levels after the match (Kılıc et al., 2019).

Another study showed that TLR2 was upregulated by 8 hours of 10-100 nM treatment with dexamethasone, another synthetic GC, which was caused by GR activation that recruited to GRE region of TLR2 promoter (Hermoso, Matsuguchi, Smoak, & Cidlowski, 2004). It was also reported that GRs which were activated after acute stress had the potential to activate not only NF-κB but also p38-MAPK or STAT signaling pathways to upregulate TLRs and IL-1β mRNA transcription (Cui et al., 2020; Shuto et al., 2002). This indicates that HC (and other GCs) may also act as mediators to enhance inflammatory response and pathogen clearance (Cruz-Topete & Cidlowski, 2015). A clinical trial including 105 septic patients revealed that concentrations of IL-1β, as well as IL-6, TNF and IFNγ, remain stably high within the first six hours after HC administration, and then start to decrease (Zhao & Ding, 2018). In addition to HC, acute treatment with dexamethasone showed similar effects regarding upregulation of pro-inflammatory genes. It was shown that LPS primed THP-1-macrophage-like cells expressed higher IL-1β mRNA and CCR7 when cells were treated with 0.1 μM dexamethasone for 24 hours, and this upregulation was inhibited after 48 hours of continuous treatment (Díez-Tercero, Delgado, & Perez, 2022). These results all indicate that short time/acute exposure to HC doesn´t suppress but rather enhance immune responses, which could be the a result of non-genomic effects of GCs activating pro-inflammatory signaling pathways.

In summary, HC acts dependent of treatment regimen both anti- and pro-inflammatory. Long-term chronic treatment suppressed pro-inflammatory NF-κB signaling pathway activation and subsequent IL-1β transcription. Acute short-term treatment on the other side seems to promote pro-inflammation to a certain degree.

4.4 NLRP3 inflammasome assembly differs between acute and chronic hydrocortisone treatment: key for regulation of IL-1β maturation

Unlike other secreted proteins, IL-1β contains no signal peptide that directs secretion via the Endoplasmic reticulum/-Golgi complex approach. The main mechanism of IL-1β secretion is its cleavage, maturation and finally release via a pore on the cell membrane (Jorgensen, Rayamajhi, & Miao, 2017). IL-1β is cleaved by caspase-1, which is activated after inflammasome assembly (Place &

Kanneganti, 2018; Stewart & Cookson, 2016). In LPS/ATP induced pyroptosis, NLRP3-inflammasome represents the major inflammasome. Its assembly is initiated by ATP and other DAMPs related to tissue injury (Kesavardhana & Kanneganti, 2017). The distinct mechanism of NLRP3-inflammasome activation by ATP remains unclear, however, potassium efflux, calcium influx, ROS formation and lysosome rupture are highly related to this process (He et al., 2016).

Chronic HC exposure resulted in a dose-dependent decrease of NLRP3 expression. Moreover, this treatment regimen inhibited inflammasome assembly and consequently reduced caspase-1 activation, gasdermin D cleavage and IL-1β release, which was accompanied by less cell death. Since pro-IL-1β levels were not affected by HC, inhibitory effects downstream of NF-κB signaling are suggested in this cascade, such as reduction of caspase-1 activation as it has been shown for other GCs (Caruso et al., 2022).

Comparable results with other GCs were widely found in other investigations. Wu et al. reported corticosterone, an analog of HC, to inhibit NLRP3 in LPS primed RAW264.7 murine macrophages by suppressing Xanthine Oxidase expression (Wu et al., 2020). In lung inflammation research, dexamethasone was found to inhibit NLRP3 expression after ovalbumin- or LPS- induced lung inflammation in mice (Guan et al., 2020; J. W. Yang et al., 2020). Results derived from these studies confirm that long-term incubation of glucocorticoids suppress NLRP3 expression and inflammasome activation. This leads to alleviation of inflammation, which mirrors the anti-inflammatory action of GCs.

As described, the effects of HC on NLRP3-inflammasome assembly and function are majorily inhibiting. However, one study demonstrated that GCs can induce NLRP3 protein expression in THP-1 macrophage-like cells by sensitizing them to extracellular ATP and thereby enhancing the ATP-mediated release of pro-inflammatory cytokines such as IL-1β (Busillo, Azzam, & Cidlowski, 2011). Results from the present study also indicate, that acute HC exposure resulted in a slight increase in NLRP3 expression and inflammasome assembly. This may sensitize macrophages against infection to limit pathogen spread.

Apart from the results that indicate opposed function of HC in pyroptosis, dependent on the treatment regimen, there are some limitation to be acknowledged: the

distinct mechanisms underlying acute HC exposure induced inflammasome activation remain unclear. Here ROS/mtROS production or potassium efflux and/or calcium influx might be involved, however, this represents a focus of future investigations.

4.5 Different hydrocortisone exposure patterns alter the viability of macrophages

One other key protein of pyroptosis is gasdermin D. Its cleavage by caspase-1 leads to oligomerization of gasdermin D proteins and pore formation in the cell membrane that allows the passage of small proteins like IL-1β. However, the gasdermin D pore is non-selective for ions and water, thus the cell is gradually ruptured by osmotic pressure changes (Kovacs & Miao, 2017). The effect of HC on caspase-1 function and gasdermin D pore formation was not extensively investigated yet. Only one report showed that treatment with 10 µM dexamethasone for 24 hours induced an upregulation of caspase-1 and gasdermin D in a myoblast cell line (Wang et al., 2021).

Results from the present study demonstrate that chronic HC exposure protected THP-1 macrophage-like cells from LPS/ATP induced pyroptosis by reduced caspase-1 activation as well as gasdermin D expression and cleavage.

Interestingly, acute HC exposure led to a different outcome. In this setting, inflammasome assembly, caspase-1 activation and IL-1β release were increased without causing higher rates of pyroptotic cell death in comparison to the physiological control. The relatively high proportion of caspase-1/PI double positive cells might be explained by PI that diffused through the gasdermin D pore rather than cell death (Evavold et al., 2018). The increased activity of caspase-1 and release of IL-1β in the acute HC setting might be attributed to inflammasome hyperactivity (Frising et al., 2022) which can be caused by GCs (Busillo et al., 2011), especially by a sudden increase at the onset of infection. Another possible explanation might be a general hyperactivation of macrophages by treatment with LPS (Crayne, Albeituni, Nichols, & Cron, 2019) that didn´t occur upon chronic HC treatment due to already inhibited signaling cascades. Hyperactivation of macrophages, in which cells release IL-1β through gasdermin D pores without dying can be also

induced by oxidized lipids (Evavold et al., 2018; Zanoni, Tan, Di Gioia, Springstead, & Kagan, 2017) and Toll-IL-1R protein SARM (Carty et al., 2019). However, for drawing conclusions, the activation state of THP-1 macrophage-like cells shall be tested in future investigations by e.g. measurement of cell surface activation markers or investigation of the p38-MAPK signaling pathway since acute HC exposure was reported to modulate this signaling pathway in a non-genomic manner (Cruz-Topete & Cidlowski, 2015).

4.6 Conclusions and perspective for application of GCs in the laboratory setting and clinic

HC is the natural form of GC in humans and can be also used as medicine, however the short biological half-life (8-12 hours) makes its application limited in clinical settings. There are several synthetic GCs or GC analogs which have more persistent effects and stronger pharmacology potency (Deng, Chalhoub, Sherwin, Li, & Brunner, 2019). Dexamethasone, for instance, is based on HC but it is methylated at 16-alpha position of D-ring and fluorinated at the 9-alpha position of B ring, which prolongs biological half-life to 36-54 hours and increases its potency to the 25-80 fold of HC. These properties make dexamethasone a more popular drug in clinical settings (Czock, Keller, Rasche, & Häussler, 2005).

As a widely used medication, HC and its GC analogs, especially dexamethasone are applied in many diseases to reduce inflammation. Asthma, the allergic inflammatory disease, can be effectively treated by GCs. GCs have been locally or systematiclly used in persistent asthma or asthma exacerbation (Derendorf, Nave, Drollmann, Cerasoli, & Wurst, 2006). HC or dexamethasone are also commonly used in autoimmune diseases like rheumatoid arthritis to suppress excess immune responses (Bluestone, 1970).

In septic shock patients, systemic inflammatory response syndrome (SIRS) represents a hallmark at the onset of disease (Feuerecker et al., 2018) and is characterized by an excessive release of pro-inflammatory cytokines which results in tissue injury, failure of single organs or multiple organ dysfunction syndrome (MODS) and further inflammation driven by DAMPs (Feuerecker et al., 2018;

Moser et al., 2022). Treatment with GCs in septic shock has the potential to improve survival of patient with SIRS (Chakraborty & Burns, 2022) and moreover, its use is recommended when fluid resuscitation and vasopressor therapy are not able to reverse hemodynamic unstability (Rhodes et al., 2017). In septic patients with acute kidney injury, HC treatment decreased 7-day cytokine levels, improved kidney function and reduced 28-day mortality rate significantly (Ying, Yang, Wu, Cai, & Xin, 2019). In Coronavirus Disease 2019 (COVID-19), GCs such as HC and dexamethasone are regarded as highly effective treatment strategies, reducing the ventilation days in patients with acute respiratory distress syndrome (ARDS) (Tomazini et al., 2020) and decreasing mortality (Angus et al., 2020; Horby et al., 2021). All these examples confirm the importance of GCs, and HC in special in the treatment of different diseases.

However, systematic and high-dose HC treatment in severely ill patients has not neglectable disadvantages with bacterial superinfection being the most common one. Superinfections or secondary infections usually occur through insufficient immune response as they are induced by long-term HC administration. IL-1β levels have been shown to be strongly suppressed upon HC treatment (Zhao & Ding, 2018), resulting in potential superinfection risk. Another side effect of HC and other GCs is central nervous system toxicity. It was found that high HC levels serve as marker for Alzheimer's disease early prediction (Ennis et al., 2017) and disease progression (de la Rubia Ortí et al., 2019). An *in vitro* study confirmed the toxicity of GCs on primary hippocampal neurons in an Alzheimer's disease animal model. A 72 hours dexamethasone treatment stimulated NLRP1 inflammasome, resulting in Aβ1-42 accumulation and IL-1β release (L. Yang et al., 2022). The neural toxicity effects of GCs have to be considered when GCs administration in diseases. These contrary results also reveal that the underlying mechanism of action of GCs in different cell types and physiological system is still unclear.

From all the clinical standards and trails, only low attention was payed to the inflammation modulating action of HC on distinct immune cells when they are infected with pathogens under acute or chronic HC treatment. The treatment reg-

imens in this *in vitro* setting strived to mimic states in patients with an acute medication with HC to treat/prevent excessive immune responses due to pathogen infection or with high stress levels or a continuous immunosuppression by HC.

The findings from the present investigations indicate that an acute exposure to high dose HC might result in an inflammasome hyperactivation leading to increased IL-1β levels and unintentionally to an excessive immune response that might in special cases ultimately contribute to a cytokine storm. In contrast, under chronic HC exposure, pyroptosis in macrophages is suppressed, leading to low release of IL-1β and consequently to a dampened immune response against infecting pathogens.

Therefore, the inclusion of IL-1β as an inflammation and pharmacological marker in clinical studies should be considered to estimate the role of HC/GC the innate immune system functional state for adjusting patients´ treatment when needed.

5. References

Alexopoulou, L., Holt, A. C., Medzhitov, R., & Flavell, R. A. (2001). Recognition of double-stranded RNA and activation of NF-kappaB by Toll-like receptor 3. *Nature, 413*(6857), 732-738. doi:10.1038/35099560

Angus, D. C., Derde, L., Al-Beidh, F., Annane, D., Arabi, Y., Beane, A., . . . Summers, C. (2020). Effect of Hydrocortisone on Mortality and Organ Support in Patients With Severe COVID-19: The REMAP-CAP COVID-19 Corticosteroid Domain Randomized Clinical Trial. *Jama, 324*(13), 1317-1329. doi:10.1001/jama.2020.17022

Ayroldi, E., Cannarile, L., Migliorati, G., Nocentini, G., Delfino, D. V., & Riccardi, C. (2012). Mechanisms of the anti-inflammatory effects of glucocorticoids: genomic and nongenomic interference with MAPK signaling pathways. *Faseb j, 26*(12), 4805-4820. doi:10.1096/fj.12-216382

Bauernfeind, F. G., Horvath, G., Stutz, A., Alnemri, E. S., MacDonald, K., Speert, D., . . . Latz, E. (2009). Cutting edge: NF-kappaB activating pattern recognition and cytokine receptors license NLRP3 inflammasome activation by regulating NLRP3 expression. *J Immunol, 183*(2), 787-791. doi:10.4049/jimmunol.0901363

Bellinghausen, I., Brand, U., Steinbrink, K., Enk, A. H., Knop, J., & Saloga, J. (2001). Inhibition of human allergic T-cell responses by IL-10-treated dendritic cells: differences from hydrocortisone-treated dendritic cells. *J Allergy Clin Immunol, 108*(2), 242-249. doi:10.1067/mai.2001.117177

Bergsbaken, T., Fink, S. L., & Cookson, B. T. (2009). Pyroptosis: host cell death and inflammation. *Nat Rev Microbiol, 7*(2), 99-109. doi:10.1038/nrmicro2070

Bishayi, B., & Ghosh, S. (2007). Immunobiological changes of in vivo glucocorticoid depleted male Swiss albino rats. *Immunobiology, 212*(1), 19-27. doi:10.1016/j.imbio.2006.08.006

Bishayi, B., Ghosh, S., & Bhanja, P. (2003). Effect of adrenalectomy on rat peritoneal macrophage response. *Acta Biol Hung, 54*(3-4), 335-346. doi:10.1556/ABiol.54.2003.3-4.11

Bluestone, R. (1970). Rheumatoid arthritis. Medical management. *Br Med J, 4*(5735), 602-604. doi:10.1136/bmj.4.5735.602

Boldizsar, F., Talaber, G., Szabo, M., Bartis, D., Palinkas, L., Nemeth, P., & Berki, T. (2010). Emerging pathways of non-genomic glucocorticoid (GC) signalling in T cells. *Immunobiology, 215*(7), 521-526. doi:10.1016/j.imbio.2009.10.003

Breuner, C. W., & Orchinik, M. (2002). Plasma binding proteins as mediators of corticosteroid action in vertebrates. *J Endocrinol, 175*(1), 99-112. doi:10.1677/joe.0.1750099

Broz, P., Pelegrín, P., & Shao, F. (2020). The gasdermins, a protein family executing cell death and inflammation. *Nat Rev Immunol, 20*(3), 143-157. doi:10.1038/s41577-019-0228-2

Busillo, J. M., Azzam, K. M., & Cidlowski, J. A. (2011). Glucocorticoids sensitize the innate immune system through regulation of the NLRP3 inflammasome. *J Biol Chem, 286*(44), 38703-38713. doi:10.1074/jbc.M111.275370

Busillo, J. M., & Cidlowski, J. A. (2013). The five Rs of glucocorticoid action during inflammation: ready, reinforce, repress, resolve, and restore. *Trends Endocrinol Metab, 24*(3), 109-119. doi:10.1016/j.tem.2012.11.005

Cain, D. W., & Cidlowski, J. A. (2017). Immune regulation by glucocorticoids. *Nat Rev Immunol, 17*(4), 233-247. doi:10.1038/nri.2017.1

Carty, M., Kearney, J., Shanahan, K. A., Hams, E., Sugisawa, R., Connolly, D., . . . Bowie, A. G. (2019). Cell Survival and Cytokine Release after Inflammasome Activation Is Regulated by the Toll-IL-1R Protein SARM. *Immunity, 50*(6), 1412-1424.e1416. doi:10.1016/j.immuni.2019.04.005

Caruso, F., Pedersen, J. Z., Incerpi, S., Kaur, S., Belli, S., Florea, R. M., & Rossi, M. (2022). Mechanism of Caspase-1 Inhibition by Four Anti-inflammatory Drugs Used in COVID-19 Treatment. *Int J Mol Sci, 23*(3). doi:10.3390/ijms23031849

Chakraborty, R. K., & Burns, B. (2022). Systemic Inflammatory Response Syndrome *StatPearls*. Treasure Island (FL): StatPearls Publishing

Crayne, C. B., Albeituni, S., Nichols, K. E., & Cron, R. Q. (2019). The Immunology of Macrophage Activation Syndrome. *Front Immunol, 10*, 119. doi:10.3389/fimmu.2019.00119

Cronstein, B. N., Kimmel, S. C., Levin, R. I., Martiniuk, F., & Weissmann, G. (1992). A mechanism for the antiinflammatory effects of corticosteroids: the glucocorticoid receptor regulates leukocyte adhesion to endothelial cells and expression of endothelial-leukocyte adhesion molecule 1 and intercellular adhesion molecule 1. *Proc Natl Acad Sci U S A, 89*(21), 9991-9995. doi:10.1073/pnas.89.21.9991

Cruz-Topete, D., & Cidlowski, J. A. (2015). One hormone, two actions: anti- and pro-inflammatory effects of glucocorticoids. *Neuroimmunomodulation, 22*(1-2), 20-32. doi:10.1159/000362724

Cui, L., Wang, Y., Wang, H., Dong, J., Li, Z., Li, J., . . . Li, J. (2020). Different effects of cortisol on pro-inflammatory gene expressions in LPS-, heat-killed E.coli-, or live E.coli-stimulated bovine endometrial epithelial cells. *BMC Vet Res, 16*(1), 9. doi:10.1186/s12917-020-2231-z

Czock, D., Keller, F., Rasche, F. M., & Häussler, U. (2005). Pharmacokinetics and pharmacodynamics of systemically administered glucocorticoids. *Clin Pharmacokinet, 44*(1), 61-98. doi:10.2165/00003088-200544010-00003

Daigneault, M., Preston, J. A., Marriott, H. M., Whyte, M. K., & Dockrell, D. H. (2010). The identification of markers of macrophage differentiation in PMA-stimulated THP-1 cells and monocyte-derived macrophages. *PLoS One, 5*(1), e8668. doi:10.1371/journal.pone.0008668

Davis, K. M., Engeland, C. G., & Murdock, K. W. (2020). Ex vivo LPS-stimulated cytokine production is associated with cortisol curves in response to acute psychosocial stress. *Psychoneuroendocrinology, 121*, 104863. doi:10.1016/j.psyneuen.2020.104863

de la Rubia Ortí, J. E., Prado-Gascó, V., Sancho Castillo, S., Julián-Rochina, M., Romero Gómez, F. J., & García-Pardo, M. P. (2019). Cortisol and IgA are Involved in the Progression of Alzheimer's Disease. A Pilot Study. *Cell Mol Neurobiol, 39*(7), 1061-1065. doi:10.1007/s10571-019-00699-z

Delaleu, N., & Bickel, M. (2004). Interleukin-1 beta and interleukin-18: regulation and activity in local inflammation. *Periodontol 2000, 35*, 42-52. doi:10.1111/j.0906-6713.2004.003569.x

Deng, J., Chalhoub, N. E., Sherwin, C. M., Li, C., & Brunner, H. I. (2019). Glucocorticoids pharmacology and their application in the treatment of childhood-onset systemic lupus erythematosus. *Semin Arthritis Rheum, 49*(2), 251-259. doi:10.1016/j.semarthrit.2019.03.010

Derendorf, H., Nave, R., Drollmann, A., Cerasoli, F., & Wurst, W. (2006). Relevance of pharmacokinetics and pharmacodynamics of inhaled corticosteroids to asthma. *Eur Respir J, 28*(5), 1042-1050. doi:10.1183/09031936.00074905

Dhabhar, F. S. (2002). Stress-induced augmentation of immune function--the role of stress hormones, leukocyte trafficking, and cytokines. *Brain Behav Immun, 16*(6), 785-798. doi:10.1016/s0889-1591(02)00036-3

Di, A., Xiong, S., Ye, Z., Malireddi, R. K. S., Kometani, S., Zhong, M., . . . Malik, A. B. (2018). The TWIK2 Potassium Efflux Channel in Macrophages Mediates NLRP3 Inflammasome-Induced Inflammation. *Immunity, 49*(1), 56-65.e54. doi:10.1016/j.immuni.2018.04.032

Diebold, S. S., Kaisho, T., Hemmi, H., Akira, S., & Reis e Sousa, C. (2004). Innate antiviral responses by means of TLR7-mediated recognition of single-stranded RNA. *Science, 303*(5663), 1529-1531. doi:10.1126/science.1093616

Díez-Tercero, L., Delgado, L. M., & Perez, R. A. (2022). Modulation of Macrophage Response by Copper and Magnesium Ions in Combination with Low Concentrations of Dexamethasone. *Biomedicines, 10*(4). doi:10.3390/biomedicines10040764

Ding, J., Wang, K., Liu, W., She, Y., Sun, Q., Shi, J., . . . Shao, F. (2016). Pore-forming activity and structural autoinhibition of the gasdermin family. *Nature, 535*(7610), 111-116. doi:10.1038/nature18590

Doitsh, G., Galloway, N. L., Geng, X., Yang, Z., Monroe, K. M., Zepeda, O., . . . Greene, W. C. (2014). Cell death by pyroptosis drives CD4 T-cell depletion in HIV-1 infection. *Nature, 505*(7484), 509-514. doi:10.1038/nature12940

Ennis, G. E., An, Y., Resnick, S. M., Ferrucci, L., O'Brien, R. J., & Moffat, S. D. (2017). Long-term cortisol measures predict Alzheimer disease risk. *Neurology, 88*(4), 371-378. doi:10.1212/wnl.0000000000003537

Evavold, C. L., Ruan, J., Tan, Y., Xia, S., Wu, H., & Kagan, J. C. (2018). The Pore-Forming Protein Gasdermin D Regulates Interleukin-1 Secretion

from Living Macrophages. *Immunity, 48*(1), 35-44 e36. doi:10.1016/j.immuni.2017.11.013

Feuerecker, M., Mayer, W., Kaufmann, I., Gruber, M., Muckenthaler, F., Yi, B., . . . Choukèr, A. (2013). A corticoid-sensitive cytokine release assay for monitoring stress-mediated immune modulation. *Clin Exp Immunol, 172*(2), 290-299. doi:10.1111/cei.12049

Feuerecker, M., Sudhoff, L., Crucian, B., Pagel, J. I., Sams, C., Strewe, C., . . . Choukèr, A. (2018). Early immune anergy towards recall antigens and mitogens in patients at onset of septic shock. *Sci Rep, 8*(1), 1754. doi:10.1038/s41598-018-19976-w

Fink, S. L., & Cookson, B. T. (2006). Caspase-1-dependent pore formation during pyroptosis leads to osmotic lysis of infected host macrophages. *Cell Microbiol, 8*(11), 1812-1825. doi:10.1111/j.1462-5822.2006.00751.x

Fitzgerald, K. A., & Kagan, J. C. (2020). Toll-like Receptors and the Control of Immunity. *Cell, 180*(6), 1044-1066. doi:10.1016/j.cell.2020.02.041

Fleit, H. B., & Kobasiuk, C. D. (1991). The human monocyte-like cell line THP-1 expresses Fc gamma RI and Fc gamma RII. *J Leukoc Biol, 49*(6), 556-565. doi:10.1002/jlb.49.6.556

Franchimont, D., Galon, J., Gadina, M., Visconti, R., Zhou, Y., Aringer, M., . . . O'Shea, J. J. (2000). Inhibition of Th1 immune response by glucocorticoids: dexamethasone selectively inhibits IL-12-induced Stat4 phosphorylation in T lymphocytes. *J Immunol, 164*(4), 1768-1774. doi:10.4049/jimmunol.164.4.1768

Frising, U. C., Ribo, S., Doglio, M. G., Malissen, B., van Loo, G., & Wullaert, A. (2022). Nlrp3 inflammasome activation in macrophages suffices for inducing autoinflammation in mice. *EMBO Rep, 23*(7), e54339. doi:10.15252/embr.202154339

Galluzzi, L., Vitale, I., Aaronson, S. A., Abrams, J. M., Adam, D., Agostinis, P., . . . Kroemer, G. (2018). Molecular mechanisms of cell death: recommendations of the Nomenclature Committee on Cell Death 2018. *Cell Death Differ, 25*(3), 486-541. doi:10.1038/s41418-017-0012-4

Ginhoux, F., & Jung, S. (2014). Monocytes and macrophages: developmental pathways and tissue homeostasis. *Nat Rev Immunol, 14*(6), 392-404. doi:10.1038/nri3671

Gordon, S., & Taylor, P. R. (2005). Monocyte and macrophage heterogeneity. *Nat Rev Immunol, 5*(12), 953-964. doi:10.1038/nri1733

Greulich, W., Wagner, M., Gaidt, M. M., Stafford, C., Cheng, Y., Linder, A., . . . Hornung, V. (2019). TLR8 Is a Sensor of RNase T2 Degradation Products. *Cell, 179*(6), 1264-1275.e1213. doi:10.1016/j.cell.2019.11.001

Gribar, S. C., Richardson, W. M., Sodhi, C. P., & Hackam, D. J. (2008). No longer an innocent bystander: epithelial toll-like receptor signaling in the development of mucosal inflammation. *Mol Med, 14*(9-10), 645-659. doi:10.2119/2008-00035.Gribar

Guan, M., Ma, H., Fan, X., Chen, X., Miao, M., & Wu, H. (2020). Dexamethasone alleviate allergic airway inflammation in mice by inhibiting the activation of NLRP3 inflammasome. *Int Immunopharmacol, 78*, 106017. doi:10.1016/j.intimp.2019.106017

Hayashi, F., Smith, K. D., Ozinsky, A., Hawn, T. R., Yi, E. C., Goodlett, D. R., . . . Aderem, A. (2001). The innate immune response to bacterial flagellin is mediated by Toll-like receptor 5. *Nature, 410*(6832), 1099-1103. doi:10.1038/35074106

He, Y., Hara, H., & Nunez, G. (2016). Mechanism and Regulation of NLRP3 Inflammasome Activation. *Trends Biochem Sci, 41*(12), 1012-1021. doi:10.1016/j.tibs.2016.09.002

Hemmi, H., Takeuchi, O., Kawai, T., Kaisho, T., Sato, S., Sanjo, H., . . . Akira, S. (2000). A Toll-like receptor recognizes bacterial DNA. *Nature, 408*(6813), 740-745. doi:10.1038/35047123

Henrick, B. M., Yao, X. D., Zahoor, M. A., Abimiku, A., Osawe, S., & Rosenthal, K. L. (2019). TLR10 Senses HIV-1 Proteins and Significantly Enhances HIV-1 Infection. *Front Immunol, 10*, 482. doi:10.3389/fimmu.2019.00482

Hermoso, M. A., Matsuguchi, T., Smoak, K., & Cidlowski, J. A. (2004). Glucocorticoids and tumor necrosis factor alpha cooperatively regulate toll-like receptor 2 gene expression. *Mol Cell Biol, 24*(11), 4743-4756. doi:10.1128/mcb.24.11.4743-4756.2004

Hersh, D., Monack, D. M., Smith, M. R., Ghori, N., Falkow, S., & Zychlinsky, A. (1999). The Salmonella invasin SipB induces macrophage apoptosis by binding to caspase-1. *Proc Natl Acad Sci U S A, 96*(5), 2396-2401.

Hohl, T. M., Rivera, A., Lipuma, L., Gallegos, A., Shi, C., Mack, M., & Pamer, E. G. (2009). Inflammatory monocytes facilitate adaptive CD4 T cell responses during respiratory fungal infection. *Cell Host Microbe, 6*(5), 470-481. doi:10.1016/j.chom.2009.10.007

Horby, P., Lim, W. S., Emberson, J. R., Mafham, M., Bell, J. L., Linsell, L., . . . Landray, M. J. (2021). Dexamethasone in Hospitalized Patients with Covid-19. *N Engl J Med, 384*(8), 693-704. doi:10.1056/NEJMoa2021436

Jakubzick, C. V., Randolph, G. J., & Henson, P. M. (2017). Monocyte differentiation and antigen-presenting functions. *Nat Rev Immunol, 17*(6), 349-362. doi:10.1038/nri.2017.28

Janssen, W. J., Barthel, L., Muldrow, A., Oberley-Deegan, R. E., Kearns, M. T., Jakubzick, C., & Henson, P. M. (2011). Fas determines differential fates of resident and recruited macrophages during resolution of acute lung injury. *Am J Respir Crit Care Med, 184*(5), 547-560. doi:10.1164/rccm.201011-1891OC

Jorgensen, I., Rayamajhi, M., & Miao, E. A. (2017). Programmed cell death as a defence against infection. *Nat Rev Immunol, 17*(3), 151-164. doi:10.1038/nri.2016.147

Kadmiel, M., & Cidlowski, J. A. (2013). Glucocorticoid receptor signaling in health and disease. *Trends Pharmacol Sci, 34*(9), 518-530. doi:10.1016/j.tips.2013.07.003

Kang, J. Y., Nan, X., Jin, M. S., Youn, S. J., Ryu, Y. H., Mah, S., . . . Lee, J. O. (2009). Recognition of lipopeptide patterns by Toll-like receptor 2-Toll-like receptor 6 heterodimer. *Immunity, 31*(6), 873-884. doi:10.1016/j.immuni.2009.09.018

Kashem, S. W., Haniffa, M., & Kaplan, D. H. (2017). Antigen-Presenting Cells in the Skin. *Annu Rev Immunol, 35*, 469-499. doi:10.1146/annurev-immunol-051116-052215

Kepp, O., Galluzzi, L., Zitvogel, L., & Kroemer, G. (2010). Pyroptosis - a cell death modality of its kind? *Eur J Immunol, 40*(3), 627-630. doi:10.1002/eji.200940160

Kesavardhana, S., & Kanneganti, T. D. (2017). Mechanisms governing inflammasome activation, assembly and pyroptosis induction. *Int Immunol, 29*(5), 201-210. doi:10.1093/intimm/dxx018

Kılıc, Y., Cetin, H. N., Sumlu, E., Pektas, M. B., Koca, H. B., & Akar, F. (2019). Effects of Boxing Matches on Metabolic, Hormonal, and Inflammatory Parameters in Male Elite Boxers. *Medicina (Kaunas), 55*(6). doi:10.3390/medicina55060288

Kohro, T., Tanaka, T., Murakami, T., Wada, Y., Aburatani, H., Hamakubo, T., & Kodama, T. (2004). A comparison of differences in the gene expression profiles of phorbol 12-myristate 13-acetate differentiated THP-1 cells and human monocyte-derived macrophage. *J Atheroscler Thromb, 11*(2), 88-97. doi:10.5551/jat.11.88

Kovacs, S. B., & Miao, E. A. (2017). Gasdermins: Effectors of Pyroptosis. *Trends Cell Biol, 27*(9), 673-684. doi:10.1016/j.tcb.2017.05.005

LaRock, C. N., & Cookson, B. T. (2013). Burning down the house: cellular actions during pyroptosis. *PLoS Pathog, 9*(12), e1003793. doi:10.1371/journal.ppat.1003793

Liden, J., Delaunay, F., Rafter, I., Gustafsson, J., & Okret, S. (1997). A new function for the C-terminal zinc finger of the glucocorticoid receptor. Repression of RelA transactivation. *J Biol Chem, 272*(34), 21467-21472. doi:10.1074/jbc.272.34.21467

Lim, H. Y., Müller, N., Herold, M. J., van den Brandt, J., & Reichardt, H. M. (2007). Glucocorticoids exert opposing effects on macrophage function dependent on their concentration. *Immunology, 122*(1), 47-53. doi:10.1111/j.1365-2567.2007.02611.x

Liu, J., Mustafa, S., Barratt, D. T., & Hutchinson, M. R. (2018). Corticosterone Preexposure Increases NF-κB Translocation and Sensitizes IL-1β Responses in BV2 Microglia-Like Cells. *Front Immunol, 9*, 3. doi:10.3389/fimmu.2018.00003

Liu, X., Zhang, Z., Ruan, J., Pan, Y., Magupalli, V. G., Wu, H., & Lieberman, J. (2016). Inflammasome-activated gasdermin D causes pyroptosis by forming membrane pores. *Nature, 535*(7610), 153-158. doi:10.1038/nature18629

Maeß, M. B., Wittig, B., Cignarella, A., & Lorkowski, S. (2014). Reduced PMA enhances the responsiveness of transfected THP-1 macrophages to

polarizing stimuli. *J Immunol Methods, 402*(1-2), 76-81. doi:10.1016/j.jim.2013.11.006

Mendoza-Cabrera, M. I., Navarro-Hernández, R. E., Santerre, A., Ortiz-Lazareno, P. C., Pereira-Suárez, A. L., & Estrada-Chávez, C. (2020). Effect of pregnancy hormone mixtures on cytokine production and surface marker expression in naïve and LPS-activated THP-1 differentiated monocytes/macrophages. *Innate Immun, 26*(2), 84-96. doi:10.1177/1753425919864658

Miao, E. A., Leaf, I. A., Treuting, P. M., Mao, D. P., Dors, M., Sarkar, A., . . . Aderem, A. (2010). Caspase-1-induced pyroptosis is an innate immune effector mechanism against intracellular bacteria. *Nat Immunol, 11*(12), 1136-1142. doi:10.1038/ni.1960

Moser, D., Feuerecker, M., Biere, K., Han, B., Hoerl, M., Schelling, G., . . . Woehrle, T. (2022). SARS-CoV-2 pneumonia and bacterial pneumonia patients differ in a second hit immune response model. *Sci Rep, 12*(1), 15485. doi:10.1038/s41598-022-17368-9

Nakanishi, K., Yoshimoto, T., Tsutsui, H., & Okamura, H. (2001). Interleukin-18 regulates both Th1 and Th2 responses. *Annu Rev Immunol, 19*, 423-474. doi:10.1146/annurev.immunol.19.1.423

Needham, B. D., & Trent, M. S. (2013). Fortifying the barrier: the impact of lipid A remodelling on bacterial pathogenesis. *Nat Rev Microbiol, 11*(7), 467-481. doi:10.1038/nrmicro3047

Netea, M. G., Simon, A., van de Veerdonk, F., Kullberg, B. J., Van der Meer, J. W., & Joosten, L. A. (2010). IL-1beta processing in host defense: beyond the inflammasomes. *PLoS Pathog, 6*(2), e1000661. doi:10.1371/journal.ppat.1000661

Orecchioni, M., Ghosheh, Y., Pramod, A. B., & Ley, K. (2019). Macrophage Polarization: Different Gene Signatures in M1(LPS+) vs. Classically and M2(LPS-) vs. Alternatively Activated Macrophages. *Front Immunol, 10*, 1084. doi:10.3389/fimmu.2019.01084

Orzalli, M. H., Prochera, A., Payne, L., Smith, A., Garlick, J. A., & Kagan, J. C. (2021). Virus-mediated inactivation of anti-apoptotic Bcl-2 family members promotes Gasdermin-E-dependent pyroptosis in barrier epithelial cells. *Immunity, 54*(7), 1447-1462.e1445. doi:10.1016/j.immuni.2021.04.012

Piemonti, L., Monti, P., Allavena, P., Sironi, M., Soldini, L., Leone, B. E., . . . Di Carlo, V. (1999). Glucocorticoids affect human dendritic cell differentiation and maturation. *J Immunol, 162*(11), 6473-6481.

Place, D. E., & Kanneganti, T. D. (2018). Recent advances in inflammasome biology. *Curr Opin Immunol, 50*, 32-38. doi:10.1016/j.coi.2017.10.011

Rahvar, A. H., Riesel, M., Graf, T., & Harbeck, B. (2019). Adrenal insufficiency treated with conventional hydrocortisone leads to elevated levels of Interleukin-6: a pilot study. *Endocrine, 64*(3), 727-729. doi:10.1007/s12020-019-01956-3

Randolph, G. J., Beaulieu, S., Lebecque, S., Steinman, R. M., & Muller, W. A. (1998). Differentiation of monocytes into dendritic cells in a model of

transendothelial trafficking. *Science, 282*(5388), 480-483. doi:10.1126/science.282.5388.480

Reily, M. M., Pantoja, C., Hu, X., Chinenov, Y., & Rogatsky, I. (2006). The GRIP1:IRF3 interaction as a target for glucocorticoid receptor-mediated immunosuppression. *Embo j, 25*(1), 108-117. doi:10.1038/sj.emboj.7600919

Rhen, T., & Cidlowski, J. A. (2005). Antiinflammatory action of glucocorticoids--new mechanisms for old drugs. *N Engl J Med, 353*(16), 1711-1723. doi:10.1056/NEJMra050541

Rhodes, A., Evans, L. E., Alhazzani, W., Levy, M. M., Antonelli, M., Ferrer, R., . . . Dellinger, R. P. (2017). Surviving Sepsis Campaign: International Guidelines for Management of Sepsis and Septic Shock: 2016. *Crit Care Med, 45*(3), 486-552. doi:10.1097/ccm.0000000000002255

Rieckmann, J. C., Geiger, R., Hornburg, D., Wolf, T., Kveler, K., Jarrossay, D., . . . Meissner, F. (2017). Social network architecture of human immune cells unveiled by quantitative proteomics. *Nat Immunol, 18*(5), 583-593. doi:10.1038/ni.3693

Rock, F. L., Hardiman, G., Timans, J. C., Kastelein, R. A., & Bazan, J. F. (1998). A family of human receptors structurally related to Drosophila Toll. *Proc Natl Acad Sci U S A, 95*(2), 588-593. doi:10.1073/pnas.95.2.588

Sampath, P., Moideen, K., Ranganathan, U. D., & Bethunaickan, R. (2018). Monocyte Subsets: Phenotypes and Function in Tuberculosis Infection. *Front Immunol, 9*, 1726. doi:10.3389/fimmu.2018.01726

Sborgi, L., Rühl, S., Mulvihill, E., Pipercevic, J., Heilig, R., Stahlberg, H., . . . Hiller, S. (2016). GSDMD membrane pore formation constitutes the mechanism of pyroptotic cell death. *Embo j, 35*(16), 1766-1778. doi:10.15252/embj.201694696

Shi, J., Zhao, Y., Wang, K., Shi, X., Wang, Y., Huang, H., . . . Shao, F. (2015). Cleavage of GSDMD by inflammatory caspases determines pyroptotic cell death. *Nature, 526*(7575), 660-665. doi:10.1038/nature15514

Shrivastava, G., Valenzuela Leon, P. C., & Calvo, E. (2020). Inflammasome Fuels Dengue Severity. *Front Cell Infect Microbiol, 10*, 489. doi:10.3389/fcimb.2020.00489

Shuto, T., Imasato, A., Jono, H., Sakai, A., Xu, H., Watanabe, T., . . . Li, J. D. (2002). Glucocorticoids synergistically enhance nontypeable Haemophilus influenzae-induced Toll-like receptor 2 expression via a negative cross-talk with p38 MAP kinase. *J Biol Chem, 277*(19), 17263-17270. doi:10.1074/jbc.M112190200

Sordi, M. B., Panahipour, L., Kargarpour, Z., & Gruber, R. (2022). Platelet-Rich Fibrin Reduces IL-1β Release from Macrophages Undergoing Pyroptosis. *Int J Mol Sci, 23*(15). doi:10.3390/ijms23158306

Stewart, M. K., & Cookson, B. T. (2016). Evasion and interference: intracellular pathogens modulate caspase-dependent inflammatory responses. *Nat Rev Microbiol, 14*(6), 346-359. doi:10.1038/nrmicro.2016.50

Tait, J. L., Aisbett, B., Hall, S. J., & Main, L. C. (2019). The inflammatory response to simulated day and night emergency alarm mobilisations. *PLoS One, 14*(6), e0218732. doi:10.1371/journal.pone.0218732

Tomazini, B. M., Maia, I. S., Cavalcanti, A. B., Berwanger, O., Rosa, R. G., Veiga, V. C., . . . Azevedo, L. C. P. (2020). Effect of Dexamethasone on Days Alive and Ventilator-Free in Patients With Moderate or Severe Acute Respiratory Distress Syndrome and COVID-19: The CoDEX Randomized Clinical Trial. *Jama, 324*(13), 1307-1316. doi:10.1001/jama.2020.17021

Tsuchiya, S., Kobayashi, Y., Goto, Y., Okumura, H., Nakae, S., Konno, T., & Tada, K. (1982). Induction of maturation in cultured human monocytic leukemia cells by a phorbol diester. *Cancer Res, 42*(4), 1530-1536.

Tsuchiya, S., Yamabe, M., Yamaguchi, Y., Kobayashi, Y., Konno, T., & Tada, K. (1980). Establishment and characterization of a human acute monocytic leukemia cell line (THP-1). *Int J Cancer, 26*(2), 171-176. doi:10.1002/ijc.2910260208

Wan, P., Zhang, S., Ruan, Z., Liu, X., Yang, G., Jia, Y., . . . Wu, J. (2022). AP-1 signaling pathway promotes pro-IL-1β transcription to facilitate NLRP3 inflammasome activation upon influenza A virus infection. *Virulence, 13*(1), 502-513. doi:10.1080/21505594.2022.2040188

Wang, L., Jiao, X. F., Wu, C., Li, X. Q., Sun, H. X., Shen, X. Y., . . . Gao, W. (2021). Trimetazidine attenuates dexamethasone-induced muscle atrophy via inhibiting NLRP3/GSDMD pathway-mediated pyroptosis. *Cell Death Discov, 7*(1), 251. doi:10.1038/s41420-021-00648-0

Whitfield, G. K., Jurutka, P. W., Haussler, C. A., & Haussler, M. R. (1999). Steroid hormone receptors: evolution, ligands, and molecular basis of biologic function. *J Cell Biochem, Suppl 32-33*, 110-122. doi:10.1002/(sici)1097-4644(1999)75:32+<110::aid-jcb14>3.0.co;2-t

Wilson, K. P., Black, J. A., Thomson, J. A., Kim, E. E., Griffith, J. P., Navia, M. A., . . . et al. (1994). Structure and mechanism of interleukin-1 beta converting enzyme. *Nature, 370*(6487), 270-275. doi:10.1038/370270a0

Wolf, A. A., Yáñez, A., Barman, P. K., & Goodridge, H. S. (2019). The Ontogeny of Monocyte Subsets. *Front Immunol, 10*, 1642. doi:10.3389/fimmu.2019.01642

Wu, L., Zhou, C., Wu, J., Chen, S., Tian, Z., & Du, Q. (2020). Corticosterone Inhibits LPS-Induced NLRP3 Inflammasome Priming in Macrophages by Suppressing Xanthine Oxidase. *Mediators Inflamm, 2020*, 6959741. doi:10.1155/2020/6959741

Yang, J. W., Mao, B., Tao, R. J., Fan, L. C., Lu, H. W., Ge, B. X., & Xu, J. F. (2020). Corticosteroids alleviate lipopolysaccharide-induced inflammation and lung injury via inhibiting NLRP3-inflammasome activation. *J Cell Mol Med, 24*(21), 12716-12725. doi:10.1111/jcmm.15849

Yang, L., Zhou, H., Huang, L., Su, Y., Kong, L., Ji, P., . . . Li, W. (2022). Stress level of glucocorticoid exacerbates neuronal damage and Aβ production through activating NLRP1 inflammasome in primary cultured hippocampal

neurons of APP-PS1 mice. *Int Immunopharmacol, 110*, 108972. doi:10.1016/j.intimp.2022.108972

Yang, S., & Zhang, L. (2004). Glucocorticoids and vascular reactivity. *Curr Vasc Pharmacol, 2*(1), 1-12. doi:10.2174/1570161043476483

Ying, P., Yang, C., Wu, X., Cai, Q., & Xin, W. (2019). Effect of hydrocortisone on the 28-day mortality of patients with septic acute kidney injury. *Ren Fail, 41*(1), 794-799. doi:10.1080/0886022x.2019.1658605

Yunna, C., Mengru, H., Lei, W., & Weidong, C. (2020). Macrophage M1/M2 polarization. *Eur J Pharmacol, 877*, 173090. doi:10.1016/j.ejphar.2020.173090

Zanoni, I., Tan, Y., Di Gioia, M., Springstead, J. R., & Kagan, J. C. (2017). By Capturing Inflammatory Lipids Released from Dying Cells, the Receptor CD14 Induces Inflammasome-Dependent Phagocyte Hyperactivation. *Immunity, 47*(4), 697-709.e693. doi:10.1016/j.immuni.2017.09.010

Zhang, P., Tsuchiya, K., Kinoshita, T., Kushiyama, H., Suidasari, S., Hatakeyama, M., . . . Suda, T. (2016). Vitamin B6 Prevents IL-1β Protein Production by Inhibiting NLRP3 Inflammasome Activation. *J Biol Chem, 291*(47), 24517-24527. doi:10.1074/jbc.M116.743815

Zhao, Y., & Ding, C. (2018). Effects of Hydrocortisone on Regulating Inflammation, Hemodynamic Stability, and Preventing Shock in Severe Sepsis Patients. *Med Sci Monit, 24*, 3612-3619. doi:10.12659/msm.906208

Apendix A:

Apendix B:

Acknowledgements

Since 2017 in September, I started to work as a doctoral candidate in the Laboratory of Translational Research ‘Stress and Immunity’, Department of Anesthesiology, Hospital of the University of Munich, Ludwig-Maximilians-University Munich under the supervision of Prof. Dr. med Alexander Choukér. The completion of the doctoral thesis is not only my effort but was realized with the help of many people. I would like to thank all people who supported me during my doctor works, without them I could not have finished my doctoral thesis.

First and foremost, I would like to thank my supervisor Prof. Dr. med Alexander Choukér who brought me to the new field of knowledge. He always inspires me and gives guide for me in the research. Thanks for giving me opportunity to work in such a motivated team and work with such an attractive topic: immunology in spaceflight, even though this is not the topic of the thesis but I will benefit from this for the rest of my research career. I believe he is the best supervisor in the world.

I have to thank Dr. rer. nat. Dominique Moser, she directly supervises my whole doctoral work. I have learned from her quite a lot, not only research techniques but attitude to science and research as well. She patiently encourages me throughout my doctoral works. I am grateful to be able to work with her these years and no doubt, she will be an excellent scientist in the near future.

I would also thank our team members, Biere Katharina and Marion Hörl. With the help of them, I could work without distraction, especially the advices for reagents. Warm supporting from them made the foreign life much easier for me in Munich.

Thanks for my friends Lianyong Han and Mengwen He. Without them, I could have not had this great time with full of memory. Their supports inspire in both academic but also daily life. It's nice to have friends like that.

I would also like to express gratitude to my parents and family for their uninterrupted supports and encouragement for the last 31 years. I hope I will be your pround and support in the next 31 years and longer.

I would like to thank China Scholarship Council for providing my financial support (No. 201706160127) for my doctoral study.

Finally, I would like to thank the Faculty of Medicine LMU and Ludiwig-Maximilli-ans-University Munich for the opportunity of studying in this world-renowned uni-versity.

Thanks to everyone who supported me!

Affidavit

LMU LUDWIG-MAXIMILIANS-UNIVERSITÄT MÜNCHEN | Promotionsbüro Medizinische Fakultät | MMRS

Affidavit

Han, Bing
Surname, first name

Forstenrieder Allee, 78/5.OG
Street

81476, Munich, Germany
Zip code, town, country

I hereby declare, that the submitted thesis entitled:

Differential effects of acute and chronic hydrocortisone treatment on pyroptosis *in vitro*

is my own work. I have only used the sources indicated and have not made unauthorized use of services of a third party. Where the work of others has been quoted or reproduced, the source is always given.

I further declare that the submitted thesis or parts thereof have not been presented as part of an examination degree to any other university.

Munich, 13.07.2023 — Bing Han

place, date — Signature doctoral candidate